



**HAL**  
open science

## Molecular simulation study on sorption and diffusion processes in polymeric pervaporation membrane materials

Dieter Hofmann, Claudia Schepers

► **To cite this version:**

Dieter Hofmann, Claudia Schepers. Molecular simulation study on sorption and diffusion processes in polymeric pervaporation membrane materials. *Molecular Simulation*, 2006, 32 (02), pp.73-84. 10.1080/08927020500474292 . hal-00514973

**HAL Id: hal-00514973**

**<https://hal.science/hal-00514973>**

Submitted on 4 Sep 2010

**HAL** is a multi-disciplinary open access archive for the deposit and dissemination of scientific research documents, whether they are published or not. The documents may come from teaching and research institutions in France or abroad, or from public or private research centers.

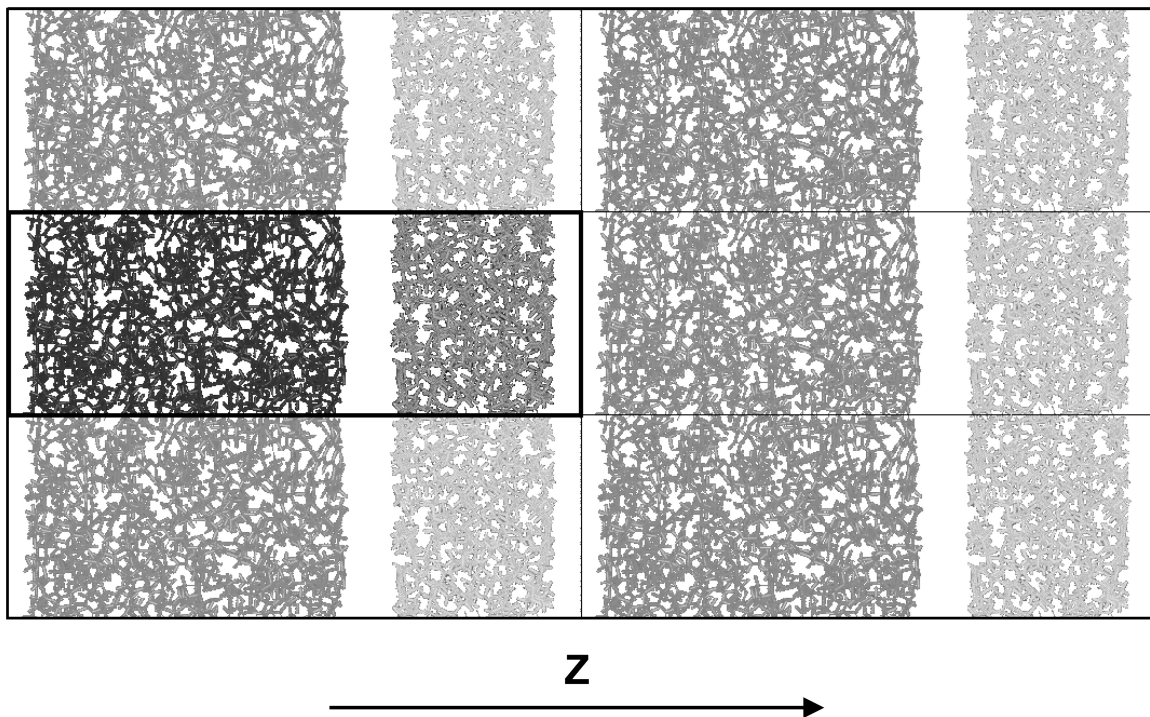
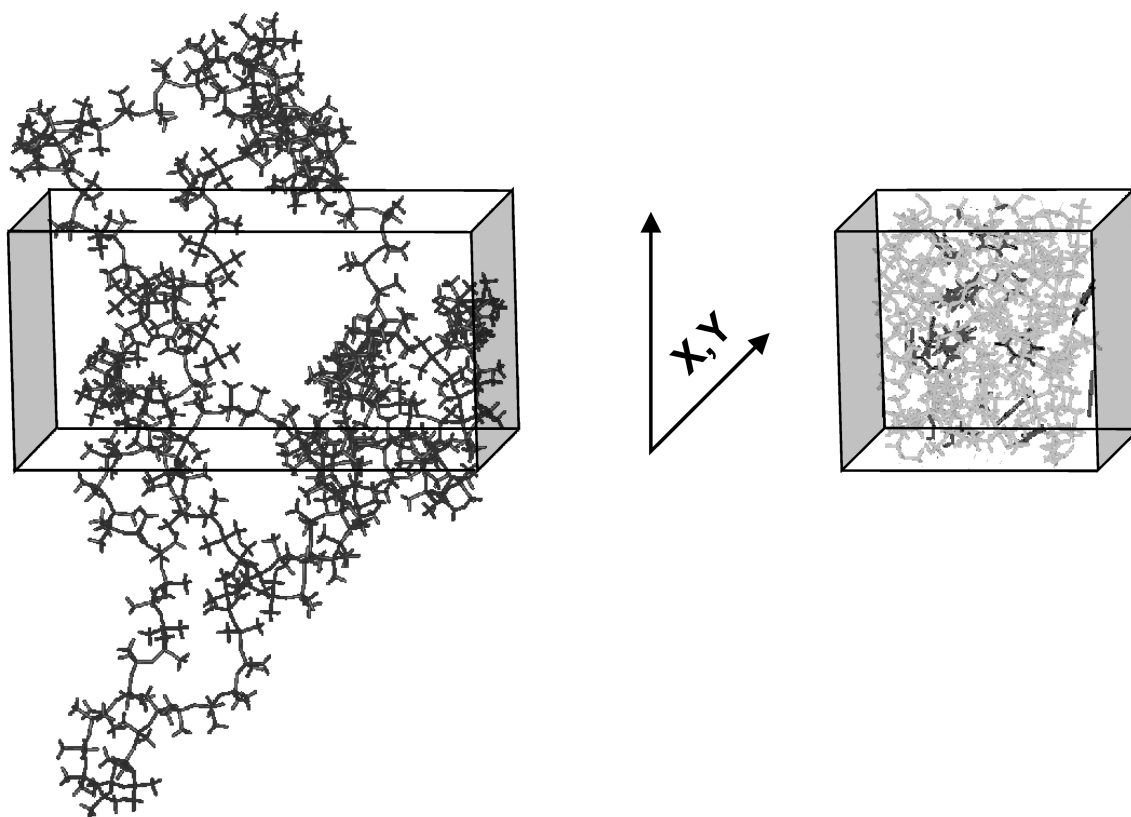
L'archive ouverte pluridisciplinaire **HAL**, est destinée au dépôt et à la diffusion de documents scientifiques de niveau recherche, publiés ou non, émanant des établissements d'enseignement et de recherche français ou étrangers, des laboratoires publics ou privés.

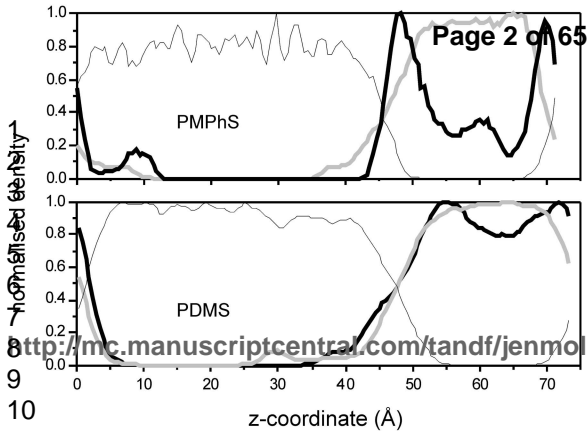
**Molecular simulation study on sorption and diffusion processes in polymeric pervaporation membrane materials**

Journal:	<i>Molecular Simulation/Journal of Experimental Nanoscience</i>
Manuscript ID:	GMOS-2005-0055.R1
Journal:	Molecular Simulation
Date Submitted by the Author:	07-Nov-2005
Complete List of Authors:	Hofmann, Dieter; GKSS Research Centre, Institute of Polymer Research Schepers, Claudia; GKSS Research Centre, Institute of Polymer Research, Institute of Polymer Research
Keywords:	Polymeric membranes, CAMM, Molecular Dynamics Simulations, Pervaporation

SCHOLARONE™  
Manuscripts

1  
2  
3  
4  
5  
6  
7  
8  
9  
10  
11  
12  
13  
14  
15  
16  
17  
18  
19  
20  
21  
22  
23  
24  
25  
26  
27  
28  
29  
30  
31  
32  
33  
34  
35  
36  
37  
38  
39  
40  
41  
42  
43  
44  
45  
46  
47  
48  
49  
50  
51  
52  
53  
54  
55  
56  
57  
58  
59  
60





normalised density

PMPHS

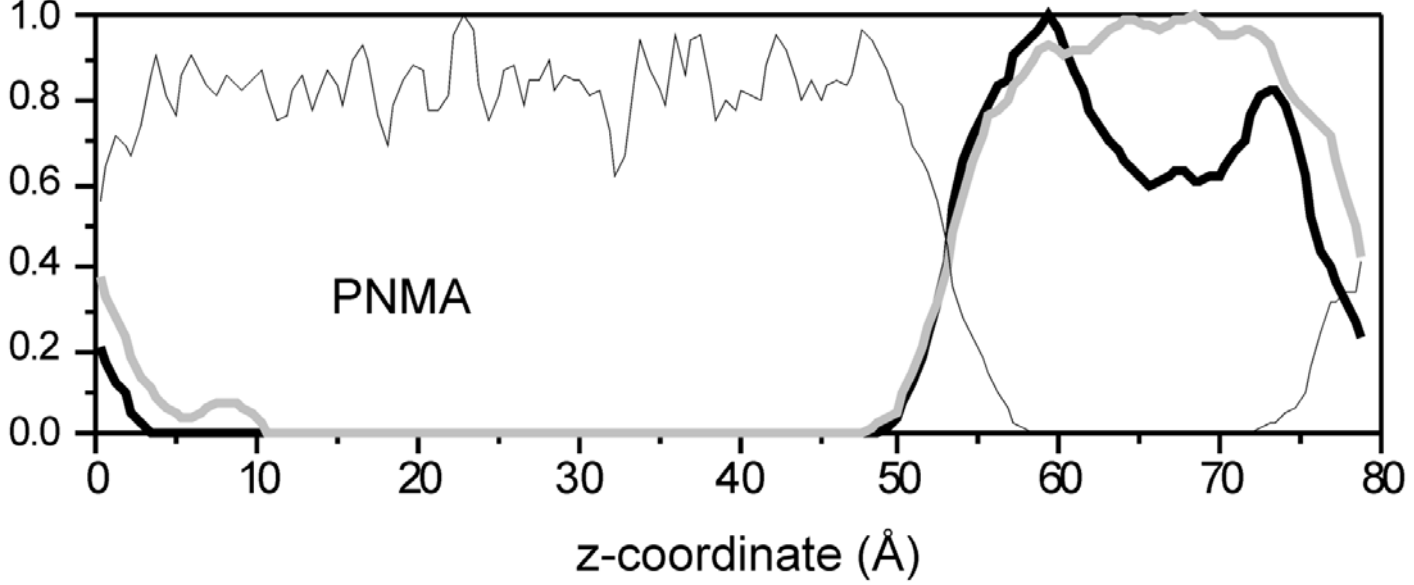
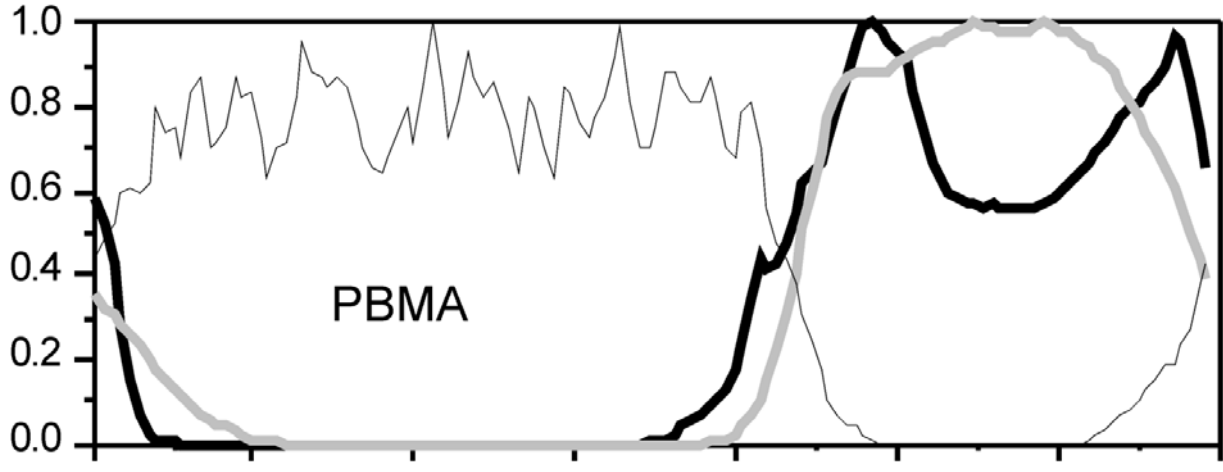
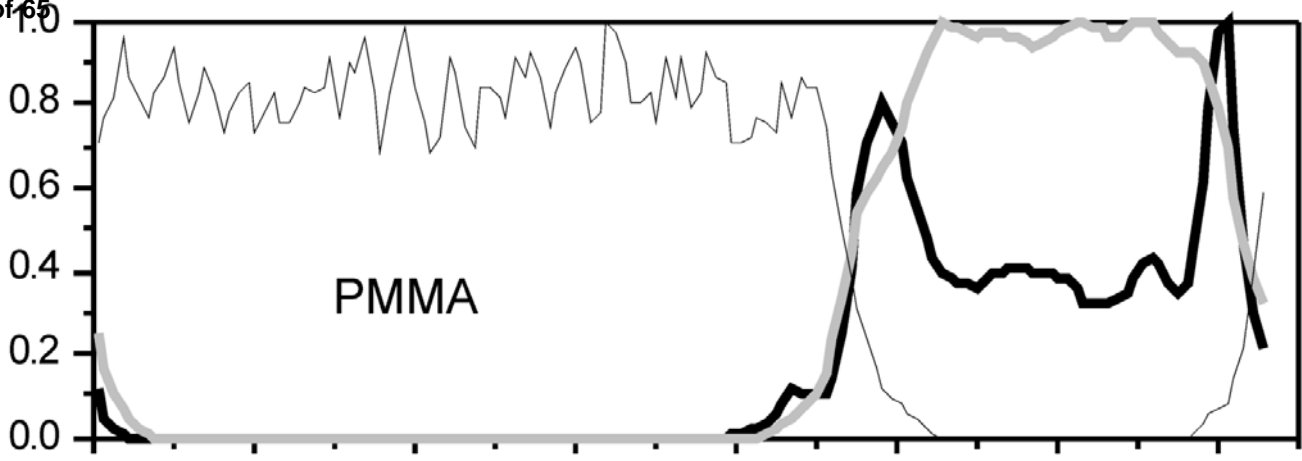
PDMS

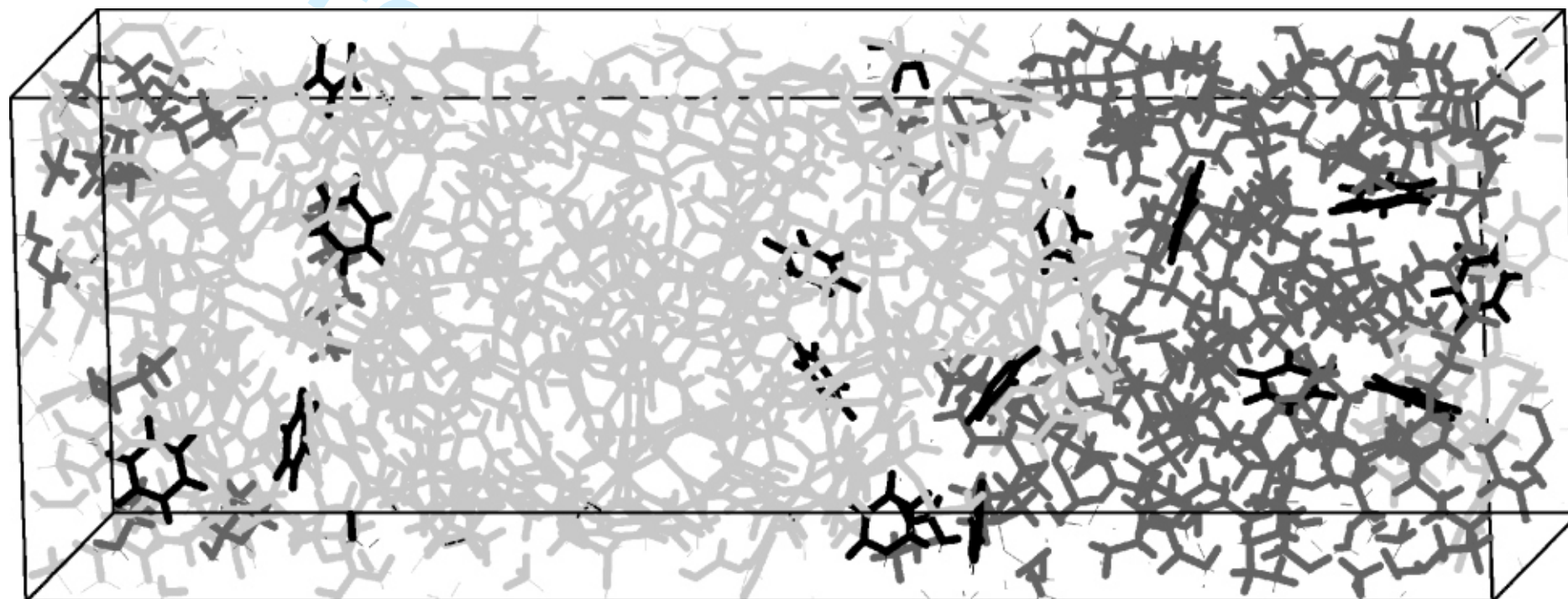
z-coordinate (Å)

<http://mc.manuscriptcentral.com/tandf/jenmol>

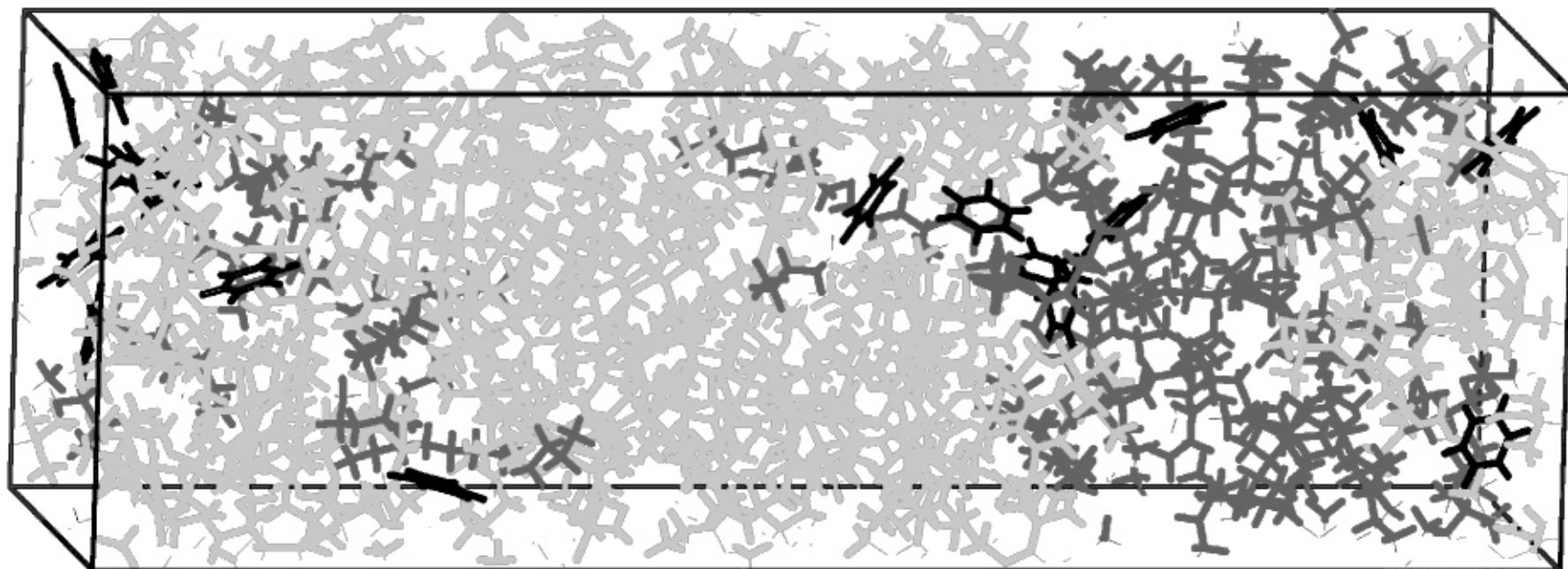
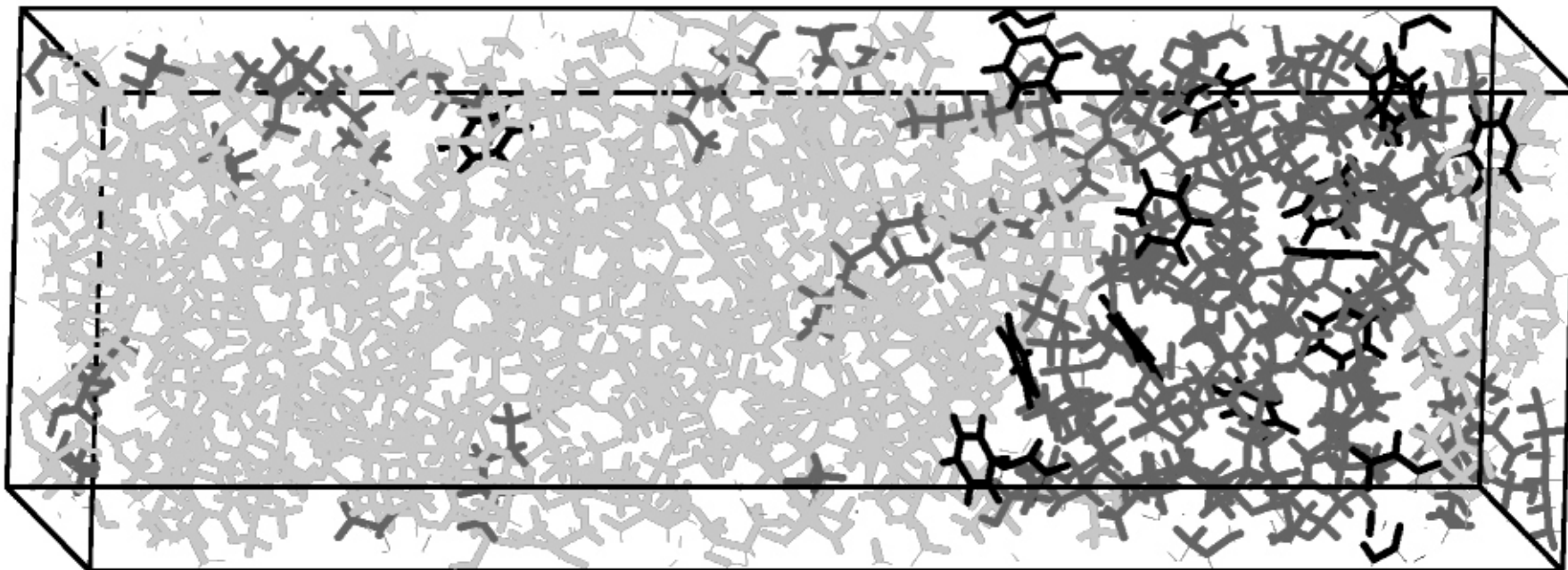
9  
10  
11

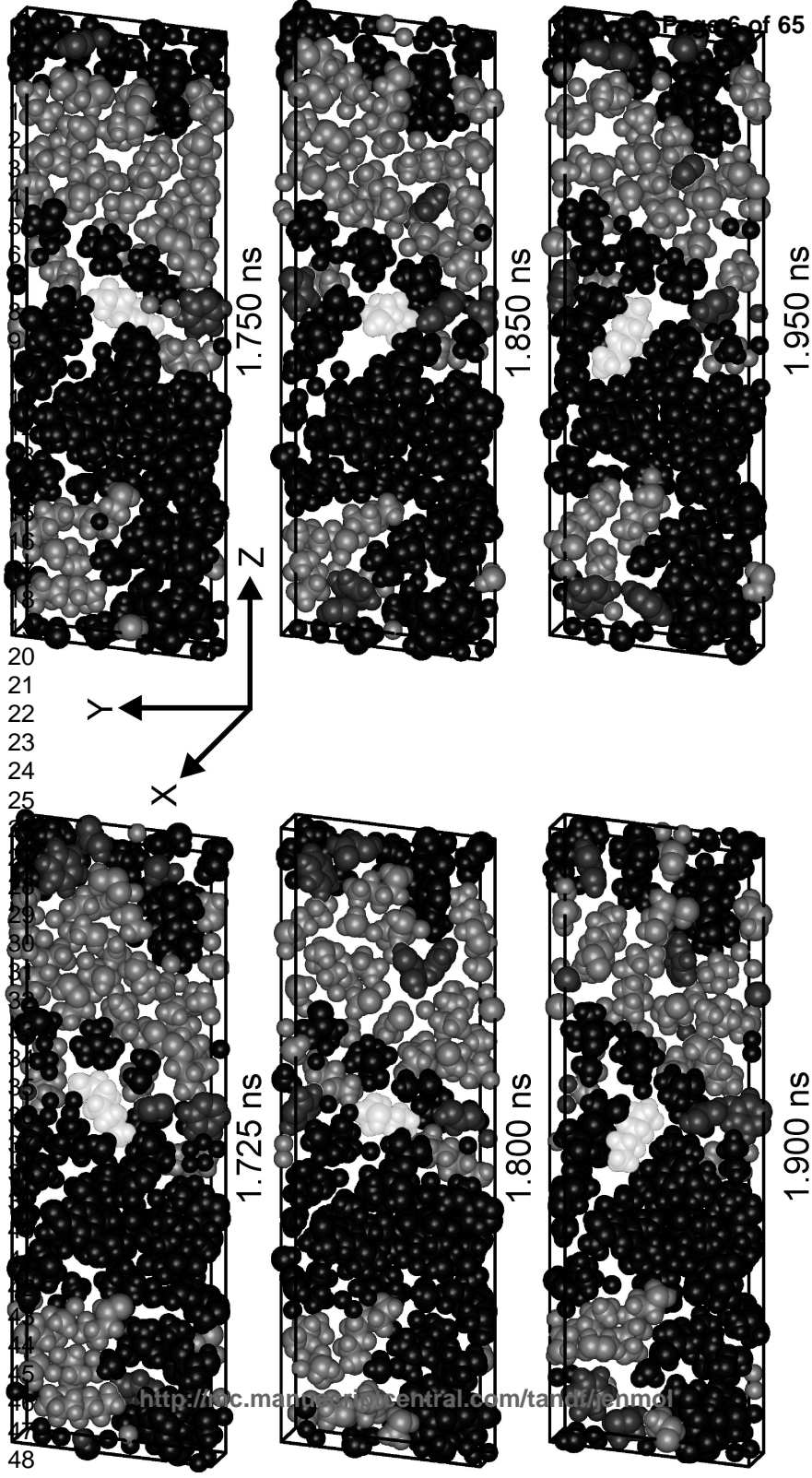
1  
2  
3  
4  
5  
6  
7  
8  
9  
10  
11  
12  
13  
14  
15  
16  
17  
18  
19  
20  
21  
22  
23  
24  
25  
26  
27  
28  
29  
30  
31  
32  
33  
34  
35  
36  
37  
38  
39  
40  
41  
42  
43  
44  
45  
46  
47  
48  
49  
50  
51  
52  
53  
54  
55  
56  
57  
58  
59  
60





1  
2  
3  
4  
5  
6  
7  
8  
9  
10  
11  
12  
13  
14  
15  
16  
17  
18  
19  
20  
21  
22  
23  
24  
25  
26  
27  
28  
29  
30  
31  
32  
33  
34  
35  
36  
37  
38  
39  
40  
41  
42  
43  
44  
45  
46  
47

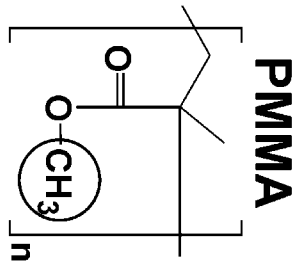




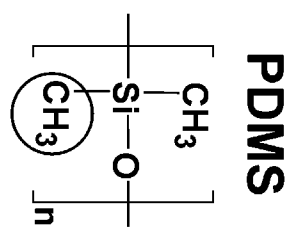


1  
2  
3  
4  
5  
6  
7  
8  
9  
10  
11  
12  
13  
14  
15  
16  
17  
18  
19  
20  
21  
22  
23  
24  
25  
26  
27  
28  
29  
30  
31  
32  
33  
34  
35  
36  
37  
38  
39  
40  
41  
42  
43  
44  
45  
46  
47  
48  
49  
50  
51  
52  
53  
54  
55  
56  
57  
58  
59  
60

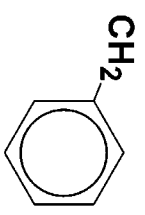
**Polymethacrylate:**



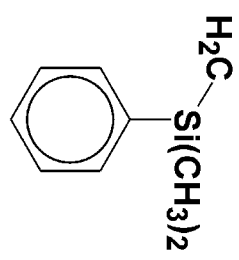
**Polysiloxane:**



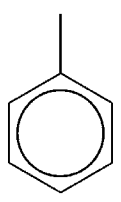
**PBMA**



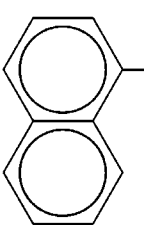
**PMPhSMA**



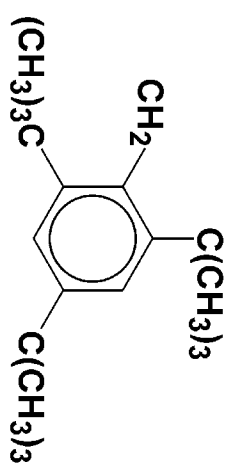
**PMPPhS**



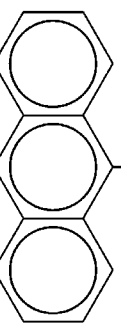
**PNMA**

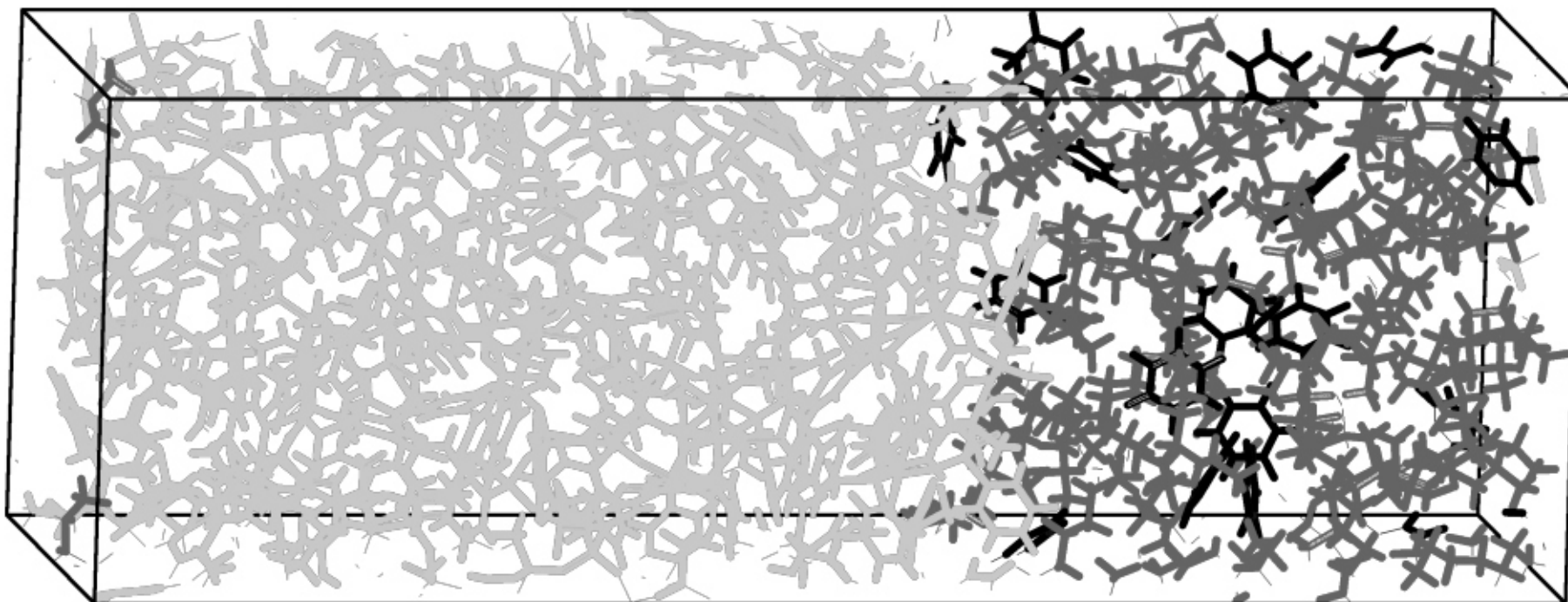


**PtBMA**



**PAMA**

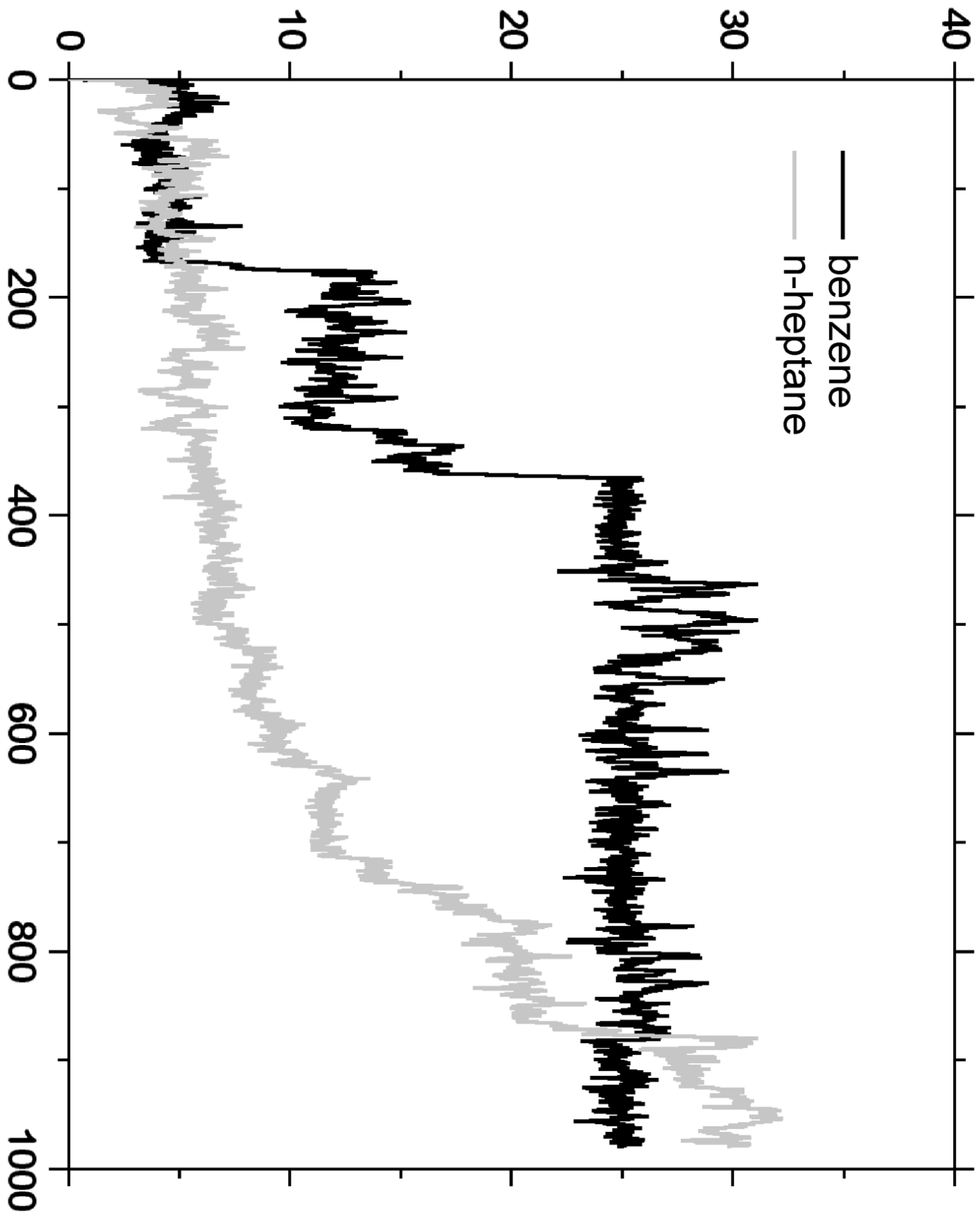




1  
2  
3  
4  
5  
6  
7  
8  
9  
10  
11  
12  
13  
14  
15  
16  
17  
18  
19  
20  
21  
22  
23  
24  
25  
26  
27  
28  
29  
30  
31  
32  
33  
34  
35  
36  
37  
38  
39  
40  
41  
42  
43  
44  
45  
46  
47

# displacement $R(t)$ in Å

1  
2  
3  
4  
5  
6  
7  
8  
9  
10  
11  
12  
13  
14  
15  
16  
17  
18  
19  
20  
21  
22  
23  
24  
25  
26  
27  
28  
29  
30  
31  
32  
33  
34  
35  
36  
37  
38  
39  
40  
41  
42  
43  
44  
45  
46  
47  
48  
49  
50  
51  
52  
53  
54  
55  
56  
57  
58  
59  
60



1  
2  
3 **Molecular simulation study on sorption and diffusion processes in polymeric**  
4 **pervaporation membrane materials**  
5  
6

7 **C. SCHEPERS, D. HOFMANN\***  
8

9  
10 GKSS Research Centre Geesthacht, Institute of Chemistry, Kantstr. 55, D-14513  
11  
12 Teltow, Germany  
13

14 **Abstract**

15  
16 Since MD simulations of membrane separation processes of aqueous/organic solutions  
17 lead to reasonable results that are in good agreement with experimental investigations  
18 an approach has been made to apply this method also for organic/organic membrane  
19 separation. In this connection the separation of a model feed mixture of 20 wt.-%  
20 benzene and 80 wt.-% n-heptane with dense amorphous polymer membranes was  
21 simulated utilising molecular modelling techniques. Special modifications of standard  
22 polymers such as polymethacrylates and polysiloxanes were investigated. It could be  
23 demonstrated that MD simulations of polymer-feed interface models can reproduce at  
24 least qualitatively important experimental results from related membrane pervaporation  
25 processes. These models are therefore suited in principle to obtain a better insight in the  
26 atomistic mechanisms of pervaporation. In addition, the knowledge about the  
27 underlying diffusion mechanism could be improved.  
28  
29  
30  
31  
32  
33  
34  
35  
36  
37  
38  
39  
40

41 **Keywords**

42  
43  
44 Polymeric membranes, Pervaporation, Molecular Dynamics Simulations, CAMM  
45  
46  
47  
48  
49  
50

---

51 \* Corresponding author, E-mail: [hofmann@gkss.de](mailto:hofmann@gkss.de), Fax: +49-3328-352452, Phone: +49-3328-352247  
52  
53

## 1. Introduction

During the last 15 years atomistic computer aided molecular modelling (CAMM) has become a widely used method for the investigation of the molecular structure of amorphous polymers and the diffusion and solubility of small molecules through these materials [cf. e.g. feature articles 1, 2]. The applied methodology of molecular dynamics (MD) simulations is based on the principles of classical mechanics and does, thus enable the handling of much larger models than quantum chemistry. Many of these simulations dealt with gas diffusion in the bulk of different rubbery and glassy polymers. In addition, there are only few papers on MD simulations in which the separation behaviour of a pervaporation membrane is described, also mainly considering the polymer bulk [cf. refs. 3-5]. It could be demonstrated that in general currently available advanced MD simulations techniques and forcefields are capable of at least qualitatively reproducing initial sorption processes at the interfacial region of polymer and solvent.

It is the main aim of this paper to describe applications of CAMM investigations which in the future may help to solve this problem for the relevant example of benzene/n-heptane mixtures by better understanding the underlying pervaporation mechanism on an atomistic scale, which are not available by any experimental method, and predictions of separation trends.

## 2. Methods

Pervaporation is an important energy saving separation technology for the separation of liquid mixtures. There, a membrane separates a liquid feed mixture (upstream side)

1  
2  
3 from a vapour phase (permeate on the downstream side), while the transport occurs in  
4 the direction of the vapour. During the separation process a phase transition occurs  
5 inside the membrane. Polymeric pervaporation membranes have hitherto mainly been  
6 used to separate (near) azeotropic mixtures of low molecular weight liquids where in  
7 most cases one component was water.  
8  
9

10  
11  
12  
13 The separation of mixtures of water and organic molecules like ethanol and methanol  
14 using pervaporation membranes is technically widely solved. In those cases also  
15 predictions made by MD simulations were found to be in good agreement with the  
16 experimental results [2]. But there is still no successful large scale commercial solution  
17 known for the pervaporation of organic/organic (like aromatic/aliphatic) liquid  
18 mixtures. This in part has to do with the fact that although major aspects of the  
19 discussed separation mechanism are determined by the static structure and the dynamic  
20 behaviour of the separation system (membrane plus penetrants) on a molecular scale, it  
21 is impossible to get sufficient direct experimental information about what is happening  
22 in these dimensions during pervaporation. Although a lot of research on pervaporation  
23 processes has been published [6-10], there is still more information needed to  
24 understand the sorption-diffusion mechanisms on the molecular level. This knowledge  
25 is particularly important for the development of membrane polymers for the  
26 pervaporation separation of organic/organic mixtures. Therefore a better basic  
27 comprehension e.g. by MD simulations is clearly wanted.  
28  
29  
30  
31  
32  
33  
34  
35  
36  
37  
38  
39  
40  
41  
42  
43  
44  
45  
46  
47  
48  
49  
50  
51  
52  
53

54  
55 The underlying separation mechanism is of the sorption-diffusion type [11]: First the  
56 molecules of the feed phase have to be selectively sorbed into the membrane at the  
57 upstream side, second diffusion through the membrane takes place and third the  
58  
59  
60

permeants get desorbed into the vapour phase at the downstream side. There the solution of a penetrant molecule species **A** in the membrane is described with the solubility parameter  $S_A$  (e.g. in g (penetrant)/ cm<sup>3</sup> (polymer)), while the solubility of species **B** of a binary mixture is  $S_B$ . The selectivity of a membrane, on the other hand, is often characterised by the separation factor  $\alpha$  [6]:

$$\alpha_{A/B} = \frac{(c_A/c_B)_{\text{permeate}}}{(c_A/c_B)_{\text{feed}}} \quad (1)$$

with  $c_A$  and  $c_B$  being the concentrations of components **A** and **B** in the respective phase. According to Fick's first law the diffusivity of the permeants is characterised with the constants of diffusion  $D_A$  (in cm<sup>2</sup>/s) and  $D_B$  respectively. The fact that in pervaporation processes besides the permeate pressure the sorptive stage at the upstream side of the membrane is often very decisive particularly for the achievable separation factors, has led the authors of the current study to an extended approach towards pervaporation systems employing interface models for the upstream polymer-feed region [12-14]. In these papers results for the pervaporation of aqueous solutions of ethanol through polysiloxane and polyvinylalcohol (PVA) were reported.

With regard to the applied MD simulation concepts it should be stressed that there only the initial stages of adsorption, absorption and diffusion near the membrane-feed interface region could be investigated, while the remarks made above on the sorption-diffusion mechanism considered macroscopic samples, where e.g. Fick's law describes a statistical transport process.

Formatted: English U.K.

### 3. Materials and simulation details

This paper presents results of new MD simulations of interface phenomena during pervaporation processes for the example of an organic/organic feed mixture. As model system for such a binary organic mixture with close boiling points a solution of 20 wt.-% benzene in 80 wt.-% n-heptane was chosen. Since, hitherto no polymeric material is known that would e.g. meet the desired selectivity  $\alpha_{\text{benzene/n-heptane}}$  of at least 10, a number of materials suggested by experimentalists [15] were subjected to respective MD simulations. The discussed results concern for instance trend predictions for the initial sorptive stage of the pervaporation at the polymer-feed interface and better insight in potential differences in the diffusion mechanisms for the conformationally rigid benzene and the conformationally rather flexible n-heptane penetrant molecules.

The investigated classes of polymers were polysiloxanes and polymethacrylates. Figure 1 contains all investigated structures. The polysiloxanes poly(dimethyl siloxane) (PDMS) and poly(methyl phenyl siloxane) (PMPHS) were included on the one hand for comparison with the mentioned foregoing successful simulations on the pervaporation of water-ethanol mixtures through these materials. On the other hand the effect of substituting one methyl group in PDMS by a benzene ring in PMPHS was of interest. In the latter highly flexible polymer the "like dissolves in like" principle should be valid. Thus, the solubility for benzene should increase in comparison to PDMS.



1  
2  
3 Due to the possibility that carboxylic (COOR) groups of polymethacrylates may serve  
4 as electrophilic targets for approaching benzene molecules, polymers containing these  
5 groups were considered by experimentalists to be promising candidates for the solution  
6 of the mentioned separation problem [15]. It was for instance known that the presence  
7 of such groups in polymers can improve the benzene selectivity in the case of  
8 benzene/cyclohexane feeds [16,17].

9  
10  
11 In addition, most of the considered modifications (PBMA, PNMA, PAMA, PtBMA and  
12 PMPHsMA) of PMMA contained aromatic rings. The series PBMA, PNMA and PAMA  
13 more specifically shows an increasing contents of aromatic sub-structures. Following  
14 the "like dissolves in like" principle which was found for low molecular weight liquid  
15 systems was to be tested whether these functional groups can enhance the benzene  
16 solubility compared with PMMA.

17  
18  
19 Another approach represents PMPHsMA, that contains electron accepting silicon-atoms  
20 which may undergo energetically favourable interactions with the  $\pi$ -electrons of  
21 benzene, a  $\pi$ -electron donor. In addition there are reports in the literature that silicone-  
22 modifications of polymers can lead to improved benzene solubilities [18].

23  
24  
25 In order to improve the diffusivity of the preferentially sorbed permeand a third aspect  
26 was to increase the free volume (space not being occupied by polymer atoms) in the  
27 polymer. Therefore PtBMA was considered which is expected to have a relatively high  
28 amount of free volume due to its bulky substituents.

29  
30  
31 [Insert Figure 1 about here]

32  
33  
34 It should be mentioned that all the described modification ideas were based either on the  
35 "like dissolves in like" principle or on quantum chemical predictions for small  
36

1  
2  
3 molecules. In polymers, however the distribution and dynamics of the free volume are  
4 also very important, which means that the relatively simple design rules used might be  
5 overlaid by other effects, e.g. due to arrangements of secondary structures. Here  
6 atomistic molecular modelling based on forcefields and Newtons equations can help to  
7 estimate whether the application of the mentioned concepts may lead to improved  
8 materials.  
9

10  
11 The InsightII/Discover software of Accelrys (former Molecular Simulations) [19] was  
12 applied for the construction and the atomistic simulations. For the potential energy  
13 calculations the pcff forcefield [20] was used. This choice was based on the positive  
14 experience made with pcff for polymer – feed interface models in the case of aqueous  
15 solutions [12-14].  
16  
17

18  
19 The density of a polymer to be modelled is an important parameter for the algorithm  
20 used to fill the basic volume element of a model with the respective chain segments.  
21 Since related experimental reference data were only available for the polymers PDMS,  
22 PMPHS, PMMA and PBMA, the densities for the other model polymers were estimated  
23 using the Synthia module of the Accelrys InsightII software. Synthia is a quantitative  
24 structure property relations programme based on semi-empirical calculations, including  
25 different atom types and bond topology of the respective polymer [21,22]. As shown in  
26  
27

28  
29 Table 1, Synthia seems to provide reasonable estimates for the polymers with available  
30 experimental density values. Therefore also the predicted data for the remaining  
31 polymers are considered appropriate for the model construction. Changes of physical  
32 properties like individual component densities and swelling that occur during the course  
33 of simulation molecular dynamics are influenced by the respective forcefield. Table 1  
34  
35  
36  
37  
38  
39  
40  
41  
42  
43  
44  
45  
46  
47  
48  
49  
50  
51  
52  
53  
54  
55  
56  
57  
58  
59  
60

Deleted: 0

Deleted: 1

1  
2  
3 also contains predicted and measured data on the glass transition temperatures  $T_g$  of the  
4  
5 polymers, which are in good agreement especially considering the measurement  
6  
7 uncertainty.  
8

9  
10 [Insert Table 1 about here]

11  
12 The construction of the single phase bulk models of amorphous polymers is described in  
13  
14 detail in ref. [6]. Therefore, here only some peculiarities for creating interface models  
15  
16 are described. The interface simulation models were composed of two sub-packing  
17  
18 models in each case, one for the respective polymer and one for the respective feed  
19  
20 mixture (cf. Figure 2).  
21

22  
23 [Insert Figure 2 about here]

24  
25 Each pure polymer box and pure feed box was packed separately utilising the  
26  
27 amorphous cell module of the InsightII software to obtain an initial guess filling with  
28  
29 chain segments or feed molecules. The basic initial packing procedure follows the  
30  
31 Theodorou-Suter algorithm [23,24]. This procedure normally assumes a three-  
32  
33 dimensional (3-D) translation symmetry. In the given case, however, the polymer  
34  
35 packing model is later to be combined with a two component liquid mixture to form the  
36  
37 interface. The lateral ( $x,y$ ) dimensions of the model have to be fixed before the actual  
38  
39 packing procedure to permit the later necessary combination with the respective other  
40  
41 component (i.e. feed or polymer) of the interface model. In the third dimension penalty  
42  
43 surface potentials (cf. Eq. 2) force the non-periodic ( $z$ ) coordinates of the constituent  
44  
45 atoms in a layer of a thickness that results from the other two box-lengths and the  
46  
47 intended density of the system. The shape of this potential term leads to prohibitively  
48  
49  
50  
51  
52  
53  
54  
55  
56  
57  
58  
59  
60

Deleted: 2

Deleted: 3

high energy penalties for atoms **i** whose  $z_i$ -coordinates come close to the minimum ( $z = 0$ ) or maximum ( $z = z_{\max}$ )  $z$ -coordinate of the basic volume element.

$$U_z = K_z \sum_i \left( \frac{1}{z_i^m} + \frac{1}{(z_i - z_{\max})^m} \right) \quad (2)$$

**m** is an even integer of at least a value of 8. **K<sub>z</sub>** is the chosen force constant which is normally selected by trial and error in a way to avoid any atom coming closer than about 1 Å to  $z = 0$  or  $z = z_{\max}$ .

Due to the presence of aromatic and non-aromatic rings in most of the investigated polymer structures, unwanted catenation or spearing of those rings does often occur if the packing procedure is performed at the experimental density. In order to avoid those unwanted effects the following specific approach was used in each case. The initial packing was performed at very low densities of less than 0.1 g/cm<sup>3</sup>. Because of the fixed dimensions of the packing model in the **x**- and **y**-directions the resulting initial packing models became very long (several 100 Å) in **z**-direction. Those models were then first equilibrated under NVT (constant atom number **N**, constant model volume **V** and constant simulation temperature **T**) conditions using sequences of static structure optimisation and MD simulations combined with forcefield parameter scaling according to stages 1-5 of table 2.

[Insert Table 2 about here]

In the subsequently necessary stages of model compression and further equilibration it had to be considered that due to the presence of penalty surface potentials the Discover software of Accelrys Inc. does not allow for reasonable pressure calculations. Therefore, in this case no NPT (**P** = constant simulation pressure) simulations at high pressure

1  
2  
3 could be utilised for the model compression towards the desired experimental density of  
4  
5 the intermediate models. Instead the stepwise compression of the model was performed  
6  
7 as follows: First in Equation (2) the strength parameter  $K_z$  was increased to a very high  
8  
9 value of up to  $10^6$  kcal\*Å<sup>m</sup>/mol. This potential pushed the polymer segments about 2  
10  
11 nm away from the bottom ( $z = 0$ ) and the top ( $z = z_{\max}$ ) layers of the model and did,  
12  
13 thus lead to a first compression. Afterwards the length of the original packing cell was  
14  
15 reduced by the amount of the resulting compression of the polymer packing in  $z$ -  
16  
17 direction followed by an adjustment of the  $z$ -coordinates of all atoms. Further  
18  
19 equilibration was then achieved by stimulated annealing (cf. stages 5-7 of Table 2). The  
20  
21 whole 3-stage procedure was repeated as often as it was necessary to reach the  
22  
23 measured or predicted density of the respective model. The resulting model geometries  
24  
25 are described in Table 3, which also contains respective data for the feed phase. This  
26  
27 table also shows that for some of the polymers two independent models were  
28  
29 constructed and simulated to get at least some idea about the reproducibility of these  
30  
31 very time consuming simulations.  
32

33  
34 [Insert Table 3 about here]

35  
36 The computer time consuming MD simulations and subsequent data evaluation were  
37  
38 mainly performed on the CRAY C916 of the Deutsches Klimarechenzentrum (DKRZ)  
39  
40 in Hamburg and two Silicon Graphics Octane workstations. For all MD data production  
41  
42 runs minimum image periodic boundary conditions with a (charge group based) cut-off  
43  
44 distance of 12 Å for all non-bond interactions were applied. This value was about the  
45  
46 longest possible cut-off radius to ensure minimum image periodic boundary conditions  
47  
48 which demand that this value must be smaller than half the shortest dimension of the  
49  
50 simulated packing model (lateral dimensions 24.5 Å). For neutral systems containing  
51  
52  
53  
54

1  
2  
3 only partial charges, charge-group based cutoffs of this size have worked quite well also  
4  
5 in foregoing studies [cf. e.g. 12-14].  
6  
7

8  
9  
10 The feed mixture models were also constructed using the amorphous cell module of the  
11 Accelrys software. There again a two-dimensionally (2-D) periodic basic volume  
12  
13 element was filled with the desired numbers of solvent molecules (cf. Table 3). The  
14  
15 molecules were inserted in random sequence at random positions and with random  
16  
17 orientations. After every insertion of a new molecule, the change of the system energy  
18  
19 was calculated. Using these data the acceptance of the respective insertion was decided  
20  
21 via the standard Metropolis criterion. Following the particle insertion procedure the  
22  
23 subsequent equilibration was achieved according to Table 4 with the last stage being  
24  
25 performed for 200 ps.  
26  
27

Deleted: MSI

28 [Insert Table 4 about here]  
29

30  
31 After the complete refinement of each individual box the polymer and the feed boxes  
32  
33 were layered onto each other along the z-axis and combined into a single simulation  
34  
35 cell. Then periodic boundary conditions are applied in all three dimensions (3D-PBC)  
36  
37 so that no energetic barriers force the atoms to remain in the given volume element.  
38  
39 Thus, the simulation cell that contains on the average 6000 atoms is only one of an  
40  
41 infinite number of periodically repeated simulation cells (cf. Figure 2). The number of  
42  
43 included molecules and the boxlengths of the layered boxes for the different polymer-  
44  
45 feed systems are listed in Table 3. Due to the influence of the penalty surface potentials  
46  
47 applied in the construction phase, immediately after the surface formation there is a  
48  
49 small empty slit of a few Å thickness between the polymer and the feed phases (cf.  
50  
51  
52  
53  
54

1  
2  
3 Figure 2). To enable a smooth approach of polymer segments and solvent molecules  
4 into these slits and towards the real system density, about 50000 steps of MD simulation  
5 were performed at 303 K with NVT ensembles at very small time steps of 0.05 - 0.1 fs.  
6  
7 The MD production runs could then be performed with a time step of 1 fs as NVT  
8 ensembles for the overall simulation times and temperatures (mostly 303 K) given in  
9 Table 3. The state of the model system, i.e. atomic positions and velocities, energy  
10 status etc., of the respective simulation runs was saved every 500 fs in a history file. In  
11 total every model simulation was carried out for up to 8ns until either steady state was  
12 reached or the feed got depleted.  
13  
14  
15  
16  
17  
18  
19  
20  
21  
22  
23  
24  
25  
26  
27  
28

#### 29 **4. Results and discussion:**

30  
31 In the case of the water/ethanol feed systems investigated earlier [12-14], the initial  
32 adsorptive behaviour of simulated interface models already gave a qualitative indication  
33 for the general separation trend to be expected during pervaporation. The interface  
34 simulations for the polysiloxanes for instance, in all cases reflected the expected  
35 preferential initial ethanol sorption. Already after 1 ns of a MD simulation the two feed  
36 components separated whereby the ethanol molecules accumulated at the respective  
37 polymer surfaces taking a favourite average orientation with the hydrophobic parts  
38 pointing in the direction of the polymer and the hydrophilic parts pointing in the  
39 direction of the water molecules. This was related with the fact that in pervaporation  
40 usually the sorption of feed molecules in the upstream top layer of a membrane is the  
41  
42  
43  
44  
45  
46  
47  
48  
49  
50  
51  
52  
53  
54  
55  
56  
57  
58  
59  
60

1  
2  
3 most decisive step of the separation process. Therefore also in the given case of the  
4 mentioned benzene/n-heptane mixture it was of interest to check possibilities for  
5 qualitative predictions of separation trends.  
6  
7  
8

Deleted: ¶

#### 9 10 **4.1 Initial Adsorption:**

11 For illustrative purposes Figure 3 shows the PMPHS-1 interface model just after the  
12 equilibration (0.1 ns MD simulation time), where the benzene molecules are still almost  
13 uniformly distributed in the feed phase.  
14  
15  
16

17 [Insert Figure 3 about here]  
18

19 To get a quantitative description of the initial adsorption of feed molecules during the  
20 further course of the MD production run normalised density profiles for the polymer  
21 repeat units and the benzene and n-heptane molecules have been calculated in the  
22 following manner: A thin slice of a few Å thickness cut perpendicular to the z-axis of  
23 the model is moved through the model along the z-axis with a small step-width (a few  
24 tenth of an Å). In each slice the centroids of polymer repeat units and the respective  
25 centroids of benzene and n-heptane molecules are counted. The resulting density  
26 distribution functions are averaged over a large number of snapshots taken for the  
27 model geometry during the MD simulations. There, due to statistical problems the  
28 averaging can only be performed until a certain number of feed molecules has been  
29 absorbed in the polymer.  
30  
31  
32  
33  
34  
35  
36  
37  
38  
39  
40  
41  
42

43 [Insert Figure 4 about here]  
44

45 Figure 4 contains the respective density profiles for the PDMS-1 and PMPHS-1 models.  
46

47 It can clearly be recognised that in the case of PDMS the simulated initial adsorptive  
48 behaviour does not indicate any significant preferential permeation of either one feed  
49  
50  
51  
52  
53  
54



1  
2  
3 component through this polymer. This is the same result as it was found experimentally  
4  
5 [27].

Deleted: 6

6  
7  
8 Now the principle of similarity would suggest that the situation towards a more  
9  
10 preferred benzene separation would improve if one of the methyl groups in each PDMS  
11  
12 repeat unit would be replaced by a benzene group. That is exactly what is indicated in  
13  
14 the upper part of Figure 4 by the density profile for PMPHS, showing a significantly  
15  
16 preferred benzene adsorption at the polymer surface.

17  
18 Examples for the benzene and n-heptane adsorption on PMMA and some of its  
19  
20 derivatives, however are shown in Figure 5.

21  
22 [Insert Figure 5 about here]

23  
24  
25 It can be seen that from this point of view and in the series shown, the best separation  
26  
27 effect would be expected for the basic glassy material PMMA. As mentioned before the  
28  
29 reason for this behaviour is most likely an attractive interaction between the carbonyl  
30  
31 groups of this polymer and the  $\pi$ -electrons of the benzene. There are also strong  
32  
33 experimental indications of a preferred adsorption of benzene on PMMA that were for  
34  
35 example observed in adsorption isotherm measurements [28]. PMMA is, however a  
36  
37 very brittle polymer which is not suited for the formation of thin membrane films  
38  
39 needed to measure permeation effects. Therefore several modifications (cf. Figure 1)  
40  
41 were attempted not only to improve the mechanical properties, but also to further  
42  
43 increase the attractive interaction with benzene. But in fact those modifications  
44  
45 obviously lead to a reduction of the carbonyl-benzene interaction, resulting in a  
46  
47 decrease of benzene affinity. Most-likely large ester groups, such as benzyl (PBMA)  
48  
49 and naphthyl (PNMA), "mask" the carbonyl groups of the respective polymers making  
50  
51  
52  
53  
54

Deleted: 7

1  
2  
3 them inaccessible for local interactions with the benzene molecules of the feed.

4  
5 Consequently, none of these modifications ~~led~~ to a more pronounced initial benzene  
6  
7 adsorption in the interface simulations.  
8  
9

Deleted: did, lead

#### 10 11 **4.2 Initial Absorption:**

12  
13 Only in three cases, PMPHS, PMPHSMA and PtBMA the available simulation time of  
14  
15 up to 8 ns was sufficient to allow a representative number of feed molecules to become  
16  
17 completely absorbed in the polymer part of the respective model (cf. [for the example of](#)  
18  
19 [PMPHS](#) Figure 6).  
20  
21

22  
23 [Insert Figure 6 about here]  
24

25  
26 In these cases it was possible to obtain an estimate for the solubility-related part of the  
27  
28 separation factor of the respective polymer for benzene by averaging over a large  
29  
30 number of available snapshots of the system taken during the MD simulation:

31  
32  $\alpha_{\text{benzene/heptane}}$  (cf. Equation 1). There the averaging was performed from the simulation  
33  
34 time step at which acceptable convergence of  $\alpha_{\text{benzene/heptane}}$  could be found. For both  
35  
36 polymers values of about 2 were obtained after sufficient simulation time. Thus, not  
37  
38 even the investigated polymer (PMPHS) with the most preferred initial adsorption of  
39  
40 Benzene or the polymer (PtBMA) which showed the fastest initial diffusion (cf. below)

41  
42 did come close to the intended target for an industrial application, which ~~is~~ at about

43  
44  $\alpha_{\text{benzene/heptane}} = 10$ .  
45  
46

47  
48 Finally some results concerning the model polymer PtBMA, which was expected to  
49  
50 contain an increased amount of free volume [\(because of the bulky C\(CH<sub>3</sub>\)<sub>3</sub> substituents\)](#)

Deleted: o

Deleted: was

Formatted: Subscript

Formatted: Subscript

1  
2  
3 shall be discussed. As can be seen in Figure 7 already after a relatively short simulation  
4 time penetrant molecules coming in from the left and right hand surface of the polymer  
5 phase almost meet each other in the middle of the polymer layer.  
6  
7  
8

9  
10 [Insert Figure 7 about here]

11  
12 This is the fastest diffusion observed amongst the materials studied (The second fastest  
13 diffusion occurred in PMPHS-1, cf. Figure 6). In addition an effect related ~~to the~~  
14 phenomenon, that in pervaporation membranes normally strong differences between  
15 pure and mixed feed transport behaviours (coupling of fluxes) exist, shall be mentioned.  
16  
17 As confirmed by the following PtBMA model simulation results coupling of fluxes can  
18 strongly influence the separation behaviour. Due to the depletion of the feed from n-  
19 heptane and strong polymer swelling (pre-conditioning) the remaining excess  
20 component may be then absorbed preferentially. In about the first ns of MD simulation  
21 time the investigated PtBMA models are n-heptane selective (cf. Figure 7 ~~(top)~~), i.e. in  
22 this time mostly n-heptane molecules are entering the polymer and cause local swelling  
23 effects. This swelling leads to laterally increased hole sizes which then permit also a  
24 larger number of benzene molecules to enter the model membrane. As result already  
25 after 2 ns the PtBMA is benzene selective (cf. Figure 7 ~~(bottom)~~). Similar effects of one  
26 feed component helping the passage of another component are often found also in gas  
27 separation membranes particularly if one of the feed constituents is CO<sub>2</sub> [29]. In order  
28 to compensate such effects in the simulations the depleted feed has to be “refilled” by  
29 substitution of the excess component with the missing component.  
30  
31  
32  
33  
34  
35  
36  
37  
38  
39  
40  
41  
42  
43  
44  
45  
46  
47  
48

Deleted: with

Deleted:

Deleted: a and Table 5

Deleted: b

Deleted: 8

#### 49 4.3 Diffusion mechanism:

1  
2  
3 In several examples differences in the diffusion behaviour between the  
4 conformationally stiff benzene and the conformationally flexible n-heptane could be  
5 observed. These effects could be best seen for the two polymer models with the fastest  
6 diffusion of penetrants (PMPHS-2 and PtBMA-2). Here, the conformationally flexible  
7 n-heptane molecules follow preferentially the course of diffusion channels with a  
8 basically continuous diffusion along the voids, while the rigid benzene molecules rather  
9 remain in suited voids for up to several hundred picoseconds. Whenever then channels  
10 between two adjacent voids are opening jump events become possible, resulting in a  
11 "jump-like" diffusion mechanism of benzene similar to the case of small molecules (e.g.  
12 H<sub>2</sub>, N<sub>2</sub>, O<sub>2</sub>) in gas separation membranes [2]. This behaviour can be well recognised  
13 from graphic displays of a travelled distance  $R(t)$  of a molecule as function of  
14 simulation time  $t$ . Figure 8 shows the typical movements of each a representative  
15 benzene and n-heptane molecule in glassy PtBMA.

Deleted: nanoseconds

16  
17  
18  
19  
20  
21  
22  
23  
24  
25  
26  
27  
28  
29  
30 [Insert Figure 8 about here]

31  
32 Using the simulation data it is also possible to visualise the reptation-like mechanism of  
33 individual n-heptane molecules. Figure 9 shows an example where an n-heptane  
34 molecule (white colour) is progressing by a transformation from a relatively extended  
35 state at a simulation time of 1.725 ns via a highly coiled state in the area of 1.800 ns to  
36 again an energetically favourable, extended configuration at 1.900 ns.

37  
38  
39  
40  
41  
42 [Insert Figure 9 about here]

## 43 44 45 **5. Summary:**

1  
2  
3 The theoretical approach towards the separation problem of an organic/organic feed  
4 mixture of 20 wt% benzene and 80 wt% n-heptane with dense amorphous polymer  
5 membranes was investigated utilising molecular modelling techniques. It could be  
6 demonstrated that MD simulations of polymer-feed interface models can reproduce at  
7 least qualitatively important experimental results from related membrane pervaporation  
8 processes. For this purpose mainly the initial adsorption of feed molecules at the  
9 polymer surface and the subsequent initial stages of absorption were considered. These  
10 models are therefore suited to obtain a better insight in the mechanisms of pervaporation  
11 on atomistic length scale. For example it was found that both size and electrostatic  
12 properties of ester groups as well as void size and distribution in the polymer strongly  
13 influence the benzene affinity of PMMA derivatives.

**Deleted:** and can even reverse the observed separation tendencies

14  
15  
16  
17  
18  
19  
20  
21  
22  
23  
24  
25  
26 However, all model polymers which were studied as membranes materials for the above  
27 mentioned separation problem did not show a trend to a sufficient selectivity for  
28 industrial applications in the MD simulations. Thus, afterwards laboratory efforts for  
29 chemical synthesis, membrane formation and characterisation of a number of these  
30 materials could be avoided.

**Deleted:** could be

31  
32  
33  
34  
35  
36 In addition, the knowledge about the underlying diffusion mechanism has been  
37 improved. It could be for instance shown that the rigid benzene penetrants diffuse in a  
38 jump-like manner between adjacent holes of the respective polymer matrix while the  
39 flexible n-heptane molecules follow a more continuous diffusion style.

**Deleted:** perform

## 46 Acknowledgements

47  
48  
49  
50  
51  
52  
53

1  
2  
3 We thank Dr. Schwarz (GKSS) and Regine Apostel (GKSS) for the pervaporation  
4 measurements on PDMS films and Christine Dannenberg (Technical University of  
5 Berlin) for the measured density values. We would like to acknowledge that parts of the  
6 work were supported by the European Commission "Growth" Program, "PERMOD –  
7 Molecular modelling for the competitive molecular design of polymer materials with  
8 controlled permeability properties.", Contract #G5RD-CT-2000-200.  
9  
10  
11  
12  
13  
14  
15  
16  
17

## 18 **References**

- 19  
20 [1] F. Müller-Plathe. Permeation of polymers - A computational  
21 approach. *Acta Polymerica*, **45**, 259 (1994).  
22  
23 [2] D. Hofmann, L. Fritz, J. Ulbrich, C. Schepers, M. Böhning. Detailed-atomistic  
24 molecular modelling of small molecule diffusion and solution processes in  
25 polymeric membrane materials. *Macromol. Theory Simul.*, **9**, 293 (2000).  
26  
27 [3] Y. Tamai, H. Tanaka, K. Nakanishi. Molecular Simulation of Permeation of  
28 Small Penetrants through Membranes. 1. Diffusion Coefficients.  
29 *Macromolecules*, **27**, 4498(1994).  
30  
31 [4] Y. Tamai, H. Tanaka, K. Nakanishi. Molecular Simulation of Permeation of  
32 Small Penetrants through Membranes. 1. Solubilities. *Macromolecules*, **28**, 2544  
33 (1995).  
34  
35 [5] F. Müller-Plathe. Diffusion of water in swollen poly(vinyl alcohol) membranes  
36 studied by molecular dynamics simulation. *J. Membrane Sci.*, **141**, 147 (1998).  
37  
38 [6] M. Wesslein, A. Heintz, R.N. Lichtenthaler. Pervaporation of liquid mixtures  
39 through Poly(Vinyl Alcohol) (PVA)-Membranes. I. Study of water containing  
40  
41  
42  
43  
44  
45  
46  
47  
48  
49  
50  
51  
52  
53  
54  
55  
56  
57  
58  
59  
60

- 1  
2  
3 binary systems with complete and partial miscibility. *J. Membrane Sci.*, **51**, 169  
4  
5 (1990).  
6  
7 [7] Huang RYM (Ed.). *Pervaporation membrane separation processes*, Elsevier  
8  
9 Science, Amsterdam (1991).  
10  
11 [8] J.M. Watson, G.S. Zhang, P.A. Payne. The diffusion mechanism in silicon  
12  
13 rubber *J. Membrane Sci.*, **73**, 55 (1992).  
14  
15 [9] T.M. Aminabhavi, R.S. Khinnavar, S.B. Harpogopad, Q.T. Nguyen, K.C.  
16  
17 Hansen. Pervaporation Separation of organic-aqueous and organic-organic  
18  
19 binary mixtures. *J. Membrane Sci.-Rev. Macromol. Chem. Phys.*, **C34(2)**, 139  
20  
21 (1994).  
22  
23 [10] J.M. Watson, P.A. Payne. A study of organic compound pervaporation through  
24  
25 silicone rubber. *J. Membrane Sci.*, **49**, 171 (1990).  
26  
27 [11] M. Mulder. *Basic Principles of Membrane Technology*. Kluwer Academic  
28  
29 Publishers, Dordrecht (1991).  
30  
31 [12] L. Fritz, D. Hofmann. Molecular dynamics simulations of the transport of water-  
32  
33 ethanol mixtures through polydimethylsiloxane membranes. *Polymer*, **38**, 1035  
34  
35 (1997).  
36  
37 [13] L. Fritz , D. Hofmann. Behaviour of water-ethanol mixtures in the interfacial  
38  
39 region of different polysiloxane membranes - a molecular dynamics simulation  
40  
41 study *Polymer*, **39**, 2531 (1998).  
42  
43 [14] D. Hofmann, L. Fritz, D. Paul. Molecular modeling of pervaporation separation  
44  
45 of binary mixtures with polymeric membranes. *J. Membrane Sci.*, **144**, 145  
46  
47 (1998), 145.  
48  
49 [15] G. Malsch (GKSS Research Center). Personal communication.  
50  
51  
52  
53  
54  
55  
56  
57  
58  
59  
60

- 1  
2  
3  
4  
5  
6  
7  
8  
9  
10  
11  
12  
13  
14  
15  
16  
17  
18  
19  
20  
21  
22  
23  
24  
25  
26  
27  
28  
29  
30  
31  
32  
33  
34  
35  
36  
37  
38  
39  
40  
41  
42  
43  
44  
45  
46  
47  
48  
49  
50  
51  
52  
53  
54  
55  
56  
57  
58  
59  
60
- [16] K. Inui, H. Okamura, T. Miyata, T. Uragami. Permeation and separation of benzene/cyclohexane mixtures through cross-linked poly(alkyl methacrylate) membranes. *J. Membrane Sci.*, **132**, 193 (1997).
- [17] K. Inui, T. Noguchi, T. Miyata, T. Uragami. Pervaporation Characteristics of Methyl Methacrylate–Methacrylic Acid Copolymer Membranes Ionically Crosslinked with Metal Ions for a Benzene/Cyclohexane Mixture. *J. Appl. Polym. Sci.*, **71**, 233 (1999).
- [18] K. Kusakabe, S. Yoneshige, S. Morooka. Separation of benzene/cyclohexane mixtures using polyurethane–silica hybrid membranes. *J. Membrane Sci.*, **149**, 29 (1998).
- [19] Molecular Simulations Inc. 1999, Computational results obtained using software programs from Molecular Simulations Inc. of San Diego-molecular mechanics calculations from Discover (Version 4.0.0p+) and graphical display using InsightII., (1999).
- [20] [H. Sun, S.J. Mumby, J.R. Maple, A.T. Hagler. An ab Initio CFF93 All-Atom Force Field for Polycarbonates. \*J. Am. Chem. Soc.\*, \*\*116\*\*, 2978 \(1994\).](#)
- [21] Polymer User Guide Synthia Section, Version 400p+, San Diego: Molecular Simulations Inc., (1999), [22] J. Bicerano. Prediction of polymer properties, Marcel Dekker, New-York (1993).
- [23] D.N. Theodorou, U.W. Suter. Detailed Molecular Structure of a Vinyl Polymer Glass. *Macromolecules*, **18**, 1467 (1985).
- [24] D.N. Theodorou, U.W. Suter. Atomistic Modeling of Mechanical Properties of Polymeric Glass. *Macromolecules*, **19**, 139 (1986).

Deleted: s

Deleted: 0

Deleted: ¶

Deleted: 1

Deleted: 2

Deleted: 3



- 1  
2  
3  
4  
5  
6  
7  
8  
9  
10  
11  
12  
13  
14  
15  
16  
17  
18  
19  
20  
21  
22  
23  
24  
25  
26  
27  
28  
29  
30  
31  
32  
33  
34  
35  
36  
37  
38  
39  
40  
41  
42  
43  
44  
45  
46  
47  
48  
49  
50  
51  
52  
53  
54  
55  
56  
57  
58  
59  
60
- [25] ABCR- Catalogue 1994/95, Research Chemicals, ABCR GmbH and Co., Karlsruhe, (1994). Deleted: 4
- [26] C. Dannenberg (Technical University of Berlin). Personal communication. Deleted: 5
- [27] H.H. Schwarz (GKSS Research Center). Personal communication. Deleted: 6
- [28] A. Wenzel, H. Yanagishita, D. Kitamoto, A. Endo, K. Haraya, T. Nakane, N. Hanai, H. Matsuda, N. Koura, H. Kamusewitz, D. Paul. Effects of preparation condition of photoinduced graft filling-polymerized membranes on pervaporation performance. *J. Membrane Sci.*, **179**, 69 (2000). Deleted: 7
- [29] C. Staudt-Bickl, W.J. Koros. Improvement of CO<sub>2</sub>/CH<sub>4</sub> separation characteristics of polyimides by chemical crosslinking. *J. Membrane Sci.*, **155**, 145 (1999). Deleted: 8

System	Simulation temperature T in K	Polymer density in g cm <sup>-3</sup>		T <sub>g, Synthia</sub> in K
		ρ <sub>exp.</sub> at 298K	ρ <sub>Synthia</sub> (T)	
PDMS	303	0,95 <sup>1</sup>	0,952	154
PMPHS	303	1,102 <sup>2</sup>	1,108	213
PMMA	303		1,157	355
PBMA	303	1,188 <sup>2</sup>	1,177	385
PNMA	303	-	1,186	406
PAMA	303	-	1,220	419
PtBMA	303	-	0,967	365
PMPHSMA	303	-	1,040	375
PMPHSMA	353	-	1,028	375

Deleted: Polymerdichte

Formatted: English U.K.

<sup>1</sup> literature data taken from ref. [25]<sup>2</sup> measured with the gradient tube method [26]

Deleted: 4

Deleted: 5

Table 1: Estimates of densities ρ<sub>Synthia</sub> (plus where available measured values ρ<sub>exp.</sub>) and glass transition temperatures T<sub>g, Synthia</sub>

stage of equilibration	status of p and T	scaling factor for conformation energy terms in the forcefield	type of nonbonded interaction energy terms in the forcefield	scaling factor for atomic radii in nonbonded interaction energy terms	Integration time step in fs
1	NVT 303K	0.001	repulsive 4th order	0.5	0.05
2	NVT 303K	0.1	repulsive 4th order	0.5	0.05
3	NVT 303K	0.1	repulsive 4th order	2/3	0.05
4	NVT 303K	1	repulsive 4th order	1	0.05
5	NVT 303 K	1	6-9 potential + Coulomb	1	0.2
6	NVT 600K	1	6-9 potential + Coulomb	1	0.5
7	NVT 303K	1	6-9 potential + Coulomb	1	1

Table 2: Typical basic equilibration procedures. The individual stages lasted between 1 ps and 5 ps.

Model System	Remarks	Number of Atoms N	Length of z axis for polymer model in Å (x,y = 24,5Å)	Length of z axis for complete polymer-feed model in Å (x,y = 24,5Å)	Simulation temperature in K	Simulation time in ns
Feed-1	benzene / n-heptane (20:80) <sup>1</sup>	1448	26,3	n.a.	303	n.a.
Feed-2	benzene / n-heptane (20:80) <sup>1</sup>	1448	28,5	n.a.	353	n.a.
PDMS	+ Feed-1	2202	47,4	73,7	303	5,0
PMPHS-1	+ Feed-1	2261	45,2	71,5	303	3,5
PMPHS-2	Continuation of PMPHS-1	2261	45,2	71,5	303	5,5
PMMA	+ Feed-1	3000	46,7	73,0	303	3,0
PBMA	+ Feed-1	2592	43,1	69,4	303	5,8
PNMA	+ Feed-1	3100	52,7	79,0	303	4,0
PAMA	+ Feed-1	3700	62,6	88,9	303	3,0
PtBMA-1	+ Feed-1	3052	49,2	75,5	303	1,0
PtBMA-2	+ Feed-1	3052	49,2	75,5	303	3,0
PMPHSMA-1	+ Feed-1	3400	62,3	88,6	303	2,0
PMPHSMA-2	+ Feed-2	3400	63,0	91,5	353	8,0

<sup>1</sup> Feed composition in wt.-%

**Deleted:** <sup>2</sup> all other models were simulated with the pcff forcefield

Table 3: Basic data for the utilised polymer and feed models. The simulation time in the last column always is meant for the respective interface model (polymer-feed).

1  
2  
3  
4  
5  
6  
7  
8  
9  
10  
11  
12  
13  
14  
15  
16  
17  
18  
19  
20  
21  
22  
23  
24  
25  
26  
27  
28  
29  
30  
31  
32  
33  
34  
35  
36  
37  
38  
39  
40  
41  
42  
43  
44  
45  
46  
47

Stage of equilibration	Scaling factor for conformation terms	Scaling factor for nonbond terms
1	0.001	0.001
2	0.1	0.001
3	1	0.001
4	1	0.1
5	1	1

Table 4: Forcefield scaling factors for the feed equilibration procedure. The integration time step was always 1 fs. The 6-9 nonbond pair interaction and the Coulomb potential of the pcff forcefield were applied.

## Figure Captions

Figure 1: Selection scheme for the simulated polymers.

Figure 2: Construction of a 3-dimensional periodic (3D-PBC) interface model from a 2-dimensional periodic (2-D PBC) polymer packing model and a 2-D PBC solvent packing model (Example PDMS and benzene/n-heptane).

Figure 3: Representative view of the PMPHS-1 interface model after 0.1 ns MD simulation. Light grey = Polymer, dark grey = n-heptane, black = benzene. The long axis of the model is directed along the z-axis.

Figure 4: Normalised density profiles for polymer repeat units (thin grey line), benzene molecules (black line) and n-heptane molecules (thick grey line) as functions of the z-coordinate (in Å) of the PDMS and PMPHS-1 interface models (cf. Figure 3). PDMS was averaged over 5 ns while PMPHS-1 was averaged over 0.3 ns

Figure 5: Normalised density profiles for polymer repeat units (thin grey line), benzene molecules (black line) and n-heptane molecules (thick grey line) as functions of the z-coordinate of the respective interface model (cf. Figure 3). PMMA averaged over 1 ns, PBMA and PBNA averaged over 2 ns

Figure 6: Representative view of the PMPHS-1 interface model after 5.5 ns MD simulation. Light grey = Polymer, dark grey = n-heptane, black = benzene. The long axis of the model is directed along the z-axis.

Figure 7: Representative view of the PtBMA-2 interface model after 1 ns (top) and after 2 ns (bottom) MD simulation. Light grey = Polymer, dark grey = n-

1  
2  
3 heptane, black = benzene. The long axis of the model is directed along the z-  
4  
5 axis.  
6

7  
8 Figure 8: Displacement  $\mathbf{R}(\mathbf{t})$  vs. simulation time  $\mathbf{t}$  for a typical benzene and a typical n-  
9  
10 heptane molecule in PtBMA.

11  
12 Figure 9: Slithering move of a n-heptane molecule in PtBMA shown in a 5 Å thick slice  
13  
14 cut out of the PtBMA-2 model perpendicular to the x-axis direction. Black =  
15  
16 Polymer, light grey = n-heptane molecule of interest, grey = other n-heptane  
17  
18 and benzene molecules.  
19  
20  
21  
22  
23  
24  
25  
26  
27  
28  
29  
30  
31  
32  
33  
34  
35  
36  
37  
38  
39  
40  
41  
42  
43  
44  
45  
46  
47  
48  
49  
50  
51  
52  
53  
54  
55  
56  
57  
58  
59  
60

1  
2  
3  
4 **Molecular simulation study on sorption and diffusion processes in polymeric**  
5 **pervaporation membrane materials**  
6  
7

8 **C. SCHEPERS, D. HOFMANN\***  
9

10 GKSS Research Centre Geesthacht, Institute of Chemistry, Kantstr. 55, D-14513  
11 Teltow, Germany  
12  
13

14  
15 **Abstract**  
16

17 Since MD simulations of membrane separation processes of aqueous/organic solutions  
18 lead to reasonable results that are in good agreement with experimental investigations  
19 an approach has been made to apply this method also for organic/organic membrane  
20 separation. In this connection the separation of a model feed mixture of 20 wt.-%  
21 benzene and 80 wt.-% n-heptane with dense amorphous polymer membranes was  
22 simulated utilising molecular modelling techniques. Special modifications of standard  
23 polymers such as polymethacrylates and polysiloxanes were investigated. It could be  
24 demonstrated that MD simulations of polymer-feed interface models can reproduce at  
25 least qualitatively important experimental results from related membrane pervaporation  
26 processes. These models are therefore suited in principle to obtain a better insight in the  
27 atomistic mechanisms of pervaporation. In addition, the knowledge about the  
28 underlying diffusion mechanism could be improved.  
29  
30  
31  
32  
33  
34  
35  
36  
37  
38  
39  
40  
41  
42

43 **Keywords**  
44

45 Polymeric membranes, Pervaporation, Molecular Dynamics Simulations, CAMM  
46  
47  
48  
49  
50  
51

52  
53 

---

\* Corresponding author, E-mail: [hofmann@gkss.de](mailto:hofmann@gkss.de), Fax: +49-3328-352452, Phone: +49-3328-352247  
54  
55



## 1. Introduction

During the last 15 years atomistic computer aided molecular modelling (CAMM) has become a widely used method for the investigation of the molecular structure of amorphous polymers and the diffusion and solubility of small molecules through these materials [cf. e.g. feature articles 1, 2]. The applied methodology of molecular dynamics (MD) simulations is based on the principles of classical mechanics and does, thus enable the handling of much larger models than quantum chemistry. Many of these simulations dealt with gas diffusion in the bulk of different rubbery and glassy polymers. In addition, there are only few papers on MD simulations in which the separation behaviour of a pervaporation membrane is described, also mainly considering the polymer bulk [cf. refs. 3-5]. It could be demonstrated that in general currently available advanced MD simulations techniques and forcefields are capable of at least qualitatively reproducing initial sorption processes at the interfacial region of polymer and solvent.

It is the main aim of this paper to describe applications of CAMM investigations which in the future may help to solve this problem for the relevant example of benzene/n-heptane mixtures by better understanding the underlying pervaporation mechanism on an atomistic scale, which are not available by any experimental method, and predictions of separation trends.

## 2. Methods

Pervaporation is an important energy saving separation technology for the separation of liquid mixtures. There, a membrane separates a liquid feed mixture (upstream side)

1  
2  
3 from a vapour phase (permeate on the downstream side), while the transport occurs in  
4 the direction of the vapour. During the separation process a phase transition occurs  
5 inside the membrane. Polymeric pervaporation membranes have hitherto mainly been  
6 used to separate (near) azeotropic mixtures of low molecular weight liquids where in  
7 most cases one component was water.  
8  
9

10  
11  
12  
13  
14 The separation of mixtures of water and organic molecules like ethanol and methanol  
15 using pervaporation membranes is technically widely solved. In those cases also  
16 predictions made by MD simulations were found to be in good agreement with the  
17 experimental results [2]. But there is still no successful large scale commercial solution  
18 known for the pervaporation of organic/organic (like aromatic/aliphatic) liquid  
19 mixtures. This in part has to do with the fact that although major aspects of the  
20 discussed separation mechanism are determined by the static structure and the dynamic  
21 behaviour of the separation system (membrane plus penetrants) on a molecular scale, it  
22 is impossible to get sufficient direct experimental information about what is happening  
23 in these dimensions during pervaporation. Although a lot of research on pervaporation  
24 processes has been published [6-10], there is still more information needed to  
25 understand the sorption-diffusion mechanisms on the molecular level. This knowledge  
26 is particularly important for the development of membrane polymers for the  
27 pervaporation separation of organic/organic mixtures. Therefore a better basic  
28 comprehension e.g. by MD simulations is clearly wanted.  
29  
30  
31  
32  
33  
34  
35  
36  
37  
38  
39  
40  
41  
42  
43  
44  
45  
46  
47

48 The underlying separation mechanism is of the sorption-diffusion type [11]: First the  
49 molecules of the feed phase have to be selectively sorbed into the membrane at the  
50 upstream side, second diffusion through the membrane takes place and third the  
51  
52  
53  
54  
55

permeants get desorbed into the vapour phase at the downstream side. There the solution of a penetrant molecule species **A** in the membrane is described with the solubility parameter  $S_A$  (e.g. in g (penetrant)/ cm<sup>3</sup> (polymer)), while the solubility of species **B** of a binary mixture is  $S_B$ . The selectivity of a membrane, on the other hand, is often characterised by the separation factor  $\alpha$  [6]:

$$\alpha_{A/B} = \frac{(c_A / c_B)_{\text{permeate}}}{(c_A / c_B)_{\text{feed}}} \quad (1)$$

with  $c_A$  and  $c_B$  being the concentrations of components **A** and **B** in the respective phase. According to Fick's first law the diffusivity of the permeants is characterised with the constants of diffusion  $D_A$  (in cm<sup>2</sup>/s) and  $D_B$  respectively. The fact that in pervaporation processes besides the permeate pressure the sorptive stage at the upstream side of the membrane is often very decisive particularly for the achievable separation factors, has led the authors of the current study to an extended approach towards pervaporation systems employing interface models for the upstream polymer-feed region [12-14]. In these papers results for the pervaporation of aqueous solutions of ethanol through polysiloxane and polyvinylalcohol (PVA) were reported.

With regard to the applied MD simulation concepts it should be stressed that there only the initial stages of adsorption, absorption and diffusion near the membrane-feed interface region could be investigated, while the remarks made above on the sorption-diffusion mechanism considered macroscopic samples, where e.g. Fick's law describes a statistical transport process.

### 3. Materials and simulation details

This paper presents results of new MD simulations of interface phenomena during pervaporation processes for the example of an organic/organic feed mixture. As model system for such a binary organic mixture with close boiling points a solution of 20 wt.-% benzene in 80 wt.-% n-heptane was chosen. Since, hitherto no polymeric material is known that would e.g. meet the desired selectivity  $\alpha_{\text{benzene/n-heptane}}$  of at least 10, a number of materials suggested by experimentalists [15] were subjected to respective MD simulations. The discussed results concern for instance trend predictions for the initial sorptive stage of the pervaporation at the polymer-feed interface and better insight in potential differences in the diffusion mechanisms for the conformationally rigid benzene and the conformationally rather flexible n-heptane penetrant molecules.

The investigated classes of polymers were polysiloxanes and polymethacrylates. Figure 1 contains all investigated structures. The polysiloxanes poly(dimethyl siloxane) (PDMS) and poly(methyl phenyl siloxane) (PMPHS) were included on the one hand for comparison with the mentioned foregoing successful simulations on the pervaporation of water-ethanol mixtures through these materials. On the other hand the effect of substituting one methyl group in PDMS by a benzene ring in PMPHS was of interest. In the latter highly flexible polymer the "like dissolves in like" principle should be valid. Thus, the solubility for benzene should increase in comparison to PDMS.

1  
2  
3  
4 Due to the possibility that carboxylic (COOR) groups of polymethacrylates may serve  
5 as electrophilic targets for approaching benzene molecules, polymers containing these  
6 groups were considered by experimentalists to be promising candidates for the solution  
7 of the mentioned separation problem [15]. It was for instance known that the presence  
8 of such groups in polymers can improve the benzene selectivity in the case of  
9 benzene/cyclohexane feeds [16,17].

10  
11  
12 In addition, most of the considered modifications (PBMA, PNMA, PAMA, PtBMA and  
13 PMPHSMA) of PMMA contained aromatic rings. The series PBMA, PNMA and PAMA  
14 more specifically shows an increasing contents of aromatic sub-structures. Following  
15 the "like dissolves in like" principle which was found for low molecular weight liquid  
16 systems was to be tested whether these functional groups can enhance the benzene  
17 solubility compared with PMMA.

18  
19  
20 Another approach represents PMPHSMA, that contains electron accepting silicone-  
21 atoms which may undergo energetically favourable interactions with the  $\pi$ -electrons of  
22 benzene, a  $\pi$ -electron donor. In addition there are reports in the literature that silicone-  
23 modifications of polymers can lead to improved benzene solubilities [18].

24  
25  
26 In order to improve the diffusivity of the preferentially sorbed permeand a third aspect  
27 was to increase the free volume (~~place-space~~ not being occupied by polymer atoms) in  
28 the polymer. Therefore PtBMA was considered which is expected to have a relatively  
29 high amount of free volume due to its bulky substituents.

30  
31  
32 [Insert Figure 1 about here]

33  
34  
35 It should be mentioned that all the described modification ideas were based either on the  
36 "like dissolves in like" principle or on quantum chemical predictions for small

1  
2  
3 molecules. In polymers, however the distribution and dynamics of the free volume are  
4  
5 also very important, which means that the relatively simple design rules used might be  
6  
7 overlaid by other effects, e.g. due to arrangements of secondary structures. Here  
8  
9 atomistic molecular modelling based on forcefields and Newtons equations can help to  
10  
11 estimate whether the application of the mentioned concepts may lead to improved  
12  
13 materials.  
14

15  
16 The InsightII/Discover software of Accelrys (former Molecular Simulations) [19] was  
17  
18 applied for the construction and the atomistic simulations. For the potential energy  
19  
20 calculations the pcff forcefield [20] was used. This choice was based on the positive  
21  
22 experience made with pcff for polymer – feed interface models in the case of aqueous  
23  
24 solutions [12-14].  
25  
26

27  
28  
29 The density of a polymer to be modelled is an important parameter for the algorithm  
30  
31 used to fill the basic volume element of a model with the respective chain segments.  
32  
33 Since related experimental reference data were only available for the polymers PDMS,  
34  
35 PMPHS, PMMA and PBMA, the densities for the other model polymers were estimated  
36  
37 using the Synthia module of the Accelrys InsightII software. Synthia is a quantitative  
38  
39 structure property relations programme based on semi-empirical calculations, including  
40  
41 different atom types and bond topology of the respective polymer [21,22]. As shown  
42  
43 in Table 1, Synthia seems to provide reasonable estimates for the polymers with  
44  
45 available experimental density values. Therefore also the predicted data for the  
46  
47 remaining polymers are considered appropriate for the model construction. Changes of  
48  
49 physical properties like individual component densities and swelling that occur during  
50  
51 the course of simulation molecular dynamics are influenced by the respective forcefield.  
52  
53  
54  
55

1  
2  
3  
4 Table 1 also contains predicted and measured data on the glass transition temperatures  
5  $T_g$  of the polymers, which are in good agreement especially considering the  
6 measurement uncertainty.  
7  
8

9  
10 [Insert Table 1 about here]  
11

12  
13 The construction of the single phase bulk models of amorphous polymers is described in  
14 detail in ref. [6]. Therefore, here only some peculiarities for creating interface models  
15 are described. The interface simulation models were composed of two sub-packing  
16 models in each case, one for the respective polymer and one for the respective feed  
17 mixture (cf. Figure 2).  
18  
19  
20  
21  
22

23 [Insert Figure 2 about here]  
24

25  
26 Each pure polymer box and pure feed box was packed separately utilising the  
27 amorphous cell module of the InsightII software to obtain an initial guess filling with  
28 chain segments or feed molecules. The basic initial packing procedure follows the  
29  
30 Theodorou-Suter algorithm [232,243]. This procedure normally assumes a three-  
31 dimensional (3-D) translation symmetry. In the given case, however, the polymer  
32 packing model is later to be combined with a two component liquid mixture to form the  
33 interface. The lateral ( $x,y$ ) dimensions of the model have to be fixed before the actual  
34 packing procedure to permit the later necessary combination with the respective other  
35 component (i.e. feed or polymer) of the interface model. In the third dimension penalty  
36 surface potentials (cf. Eq. 2) force the non-periodic ( $z$ ) coordinates of the constituent  
37 atoms in a layer of a thickness that results from the other two box-lengths and the  
38 intended density of the system. The shape of this potential term leads to prohibitively  
39  
40  
41  
42  
43  
44  
45  
46  
47  
48  
49  
50  
51  
52  
53  
54  
55

high energy penalties for atoms  $i$  whose  $z_i$ -coordinates come close to the minimum ( $z = 0$ ) or maximum ( $z = z_{\max}$ )  $z$ -coordinate of the basic volume element.

$$U_z = K_z \sum_i \left( \frac{1}{z_i^m} + \frac{1}{(z_i - z_{\max})^m} \right) \quad (2)$$

$m$  is an even integer of at least a value of 8.  $K_z$  is the chosen force constant which is normally selected by trial and error in a way to avoid any atom coming closer than about 1 Å to  $z = 0$  or  $z = z_{\max}$ .

Due to the presence of aromatic and non-aromatic rings in most of the investigated polymer structures, unwanted catenation or spearing of those rings does often occur if the packing procedure is performed at the experimental density. In order to avoid those unwanted effects the following specific approach was used in each case. The initial packing was performed at very low densities of less than 0.1 g/cm<sup>3</sup>. Because of the fixed dimensions of the packing model in the  $x$ - and  $y$ -directions the resulting initial packing models became very long (several 100 Å) in  $z$ -direction. Those models were then first equilibrated under NVT (constant atom number  $N$ , constant model volume  $V$  and constant simulation temperature  $T$ ) conditions using sequences of static structure optimisation and MD simulations combined with forcefield parameter scaling according to stages 1-5 of table 2.

[Insert Table 2 about here]

In the subsequently necessary stages of model compression and further equilibration it had to be considered that due to the presence of penalty surface potentials the Discover software of Accelrys Inc. does not allow for reasonable pressure calculations. Therefore, in this case no NPT ( $P$  = constant simulation pressure) simulations at high pressure



1  
2  
3  
4 could be utilised for the model compression towards the desired experimental density of  
5  
6 the intermediate models. Instead the stepwise compression of the model was performed  
7  
8 as follows: First in Equation (2) the strength parameter  $K_z$  was increased to a very high  
9  
10 value of up to  $10^6$  kcal\*Å<sup>m</sup>/mol. This potential pushed the polymer segments about 2  
11  
12 nm away from the bottom ( $z = 0$ ) and the top ( $z = z_{\max}$ ) layers of the model and did,  
13  
14 thus lead to a first compression. Afterwards the length of the original packing cell was  
15  
16 reduced by the amount of the resulting compression of the polymer packing in  $z$ -  
17  
18 direction followed by an adjustment of the  $z$ -coordinates of all atoms. Further  
19  
20 equilibration was then achieved by stimulated annealing (cf. stages 5-7 of Table 2). The  
21  
22 whole 3-stage procedure was repeated as often as it was necessary to reach the  
23  
24 measured or predicted density of the respective model. The resulting model geometries  
25  
26 are described in Table 3, which also contains respective data for the feed phase. This  
27  
28 table also shows that for some of the polymers two independent models were  
29  
30 constructed and simulated to get at least some idea about the reproducibility of these  
31  
32 very time consuming simulations.  
33

34  
35 [Insert Table 3 about here]

36  
37 The computer time consuming MD simulations and subsequent data evaluation were  
38  
39 mainly performed on the CRAY C916 of the Deutsches Klimarechenzentrum (DKRZ)  
40  
41 in Hamburg and two Silicon Graphics Octane workstations. For all MD data production  
42  
43 runs minimum image periodic boundary conditions with a (charge group based) cut-off  
44  
45 distance of 12 Å for all non-bond interactions were applied. This value was about the  
46  
47 longest possible cut-off radius to ensure minimum image periodic boundary conditions  
48  
49 which demand that this value must be smaller than half the shortest dimension of the  
50  
51 simulated packing model (lateral dimensions 24.5 Å). For neutral systems containing  
52  
53

1  
2  
3  
4 only partial charges, charge-group based cutoffs of this size have worked quite well also  
5 in foregoing studies [cf. e.g. 12-14].  
6  
7  
8  
9

10  
11 The feed mixture models were also constructed using the amorphous cell module of the  
12 MSI-Accelrys software. There again a two-dimensionally (2-D) periodic basic volume  
13 element was filled with the desired numbers of solvent molecules (cf. Table 3). The  
14 molecules were inserted in random sequence at random positions and with random  
15 orientations. After every insertion of a new molecule, the change of the system energy  
16 was calculated. Using these data the acceptance of the respective insertion was decided  
17 via the standard Metropolis criterion. Following the particle insertion procedure the  
18 subsequent equilibration was achieved according to Table 4 with the last stage being  
19 performed for 200 ps.  
20  
21  
22  
23  
24  
25  
26  
27  
28

29 [Insert Table 4 about here]  
30  
31

32 After the complete refinement of each individual box the polymer and the feed boxes  
33 were layered onto each other along the z-axis and combined into a single simulation  
34 cell. Then periodic boundary conditions are applied in all three dimensions (3D-PBC)  
35 so that no energetic barriers force the atoms to remain in the given volume element.  
36 Thus, the simulation cell that contains on the average 6000 atoms is only one of an  
37 infinite number of periodically repeated simulation cells (cf. Figure 2). The number of  
38 included molecules and the boxlengths of the layered boxes for the different polymer-  
39 feed systems are listed in Table 3. Due to the influence of the penalty surface potentials  
40 applied in the construction phase, immediately after the surface formation there is a  
41 small empty slit of a few Å thickness between the polymer and the feed phases (cf.  
42  
43  
44  
45  
46  
47  
48  
49  
50  
51  
52  
53  
54  
55

1  
2  
3  
4 Figure 2). To enable a smooth approach of polymer segments and solvent molecules  
5 into these slits and towards the real system density, about 50000 steps of MD simulation  
6 were performed at 303 K with NVT ensembles at very small time steps of 0.05 - 0.1 fs.  
7  
8 The MD production runs could then be performed with a time step of 1 fs as NVT  
9 ensembles for the overall simulation times and temperatures (mostly 303 K) given in  
10 Table 3. The state of the model system, i.e. atomic positions and velocities, energy  
11 status etc., of the respective simulation runs was saved every 500 fs in a history file. In  
12 total every model simulation was carried out for up to 8ns until either steady state was  
13 reached or the feed got depleted.  
14  
15  
16  
17  
18  
19  
20  
21  
22  
23  
24  
25  
26  
27  
28  
29

#### 30 **4. Results and discussion:**

31  
32 In the case of the water/ethanol feed systems investigated earlier [12-14], the initial  
33 adsorptive behaviour of simulated interface models already gave a qualitative indication  
34 for the general separation trend to be expected during pervaporation. The interface  
35 simulations for the polysiloxanes for instance, in all cases reflected the expected  
36 preferential initial ethanol sorption. Already after 1 ns of a MD simulation the two feed  
37 components separated whereby the ethanol molecules accumulated at the respective  
38 polymer surfaces taking a favourite average orientation with the hydrophobic parts  
39 pointing in the direction of the polymer and the hydrophilic parts pointing in the  
40 direction of the water molecules. This was related with the fact that in pervaporation  
41 usually the sorption of feed molecules in the upstream top layer of a membrane is the  
42  
43  
44  
45  
46  
47  
48  
49  
50  
51  
52  
53  
54  
55  
56  
57  
58  
59  
60

1  
2  
3 most decisive step of the separation process. Therefore also in the given case of the  
4 mentioned benzene/n-heptane mixture it was of interest to check possibilities for  
5 qualitative predictions of separation trends.  
6  
7  
8  
9

#### 10 11 12 13 **4.1 Initial Adsorption:**

14  
15 For illustrative purposes Figure 3 shows the PMPHS-1 interface model just after the  
16 equilibration (0.1 ns MD simulation time), where the benzene molecules are still almost  
17 uniformly distributed in the feed phase.  
18  
19

20  
21  
22 [Insert Figure 3 about here]  
23

24 To get a quantitative description of the initial adsorption of feed molecules during the  
25 further course of the MD production run normalised density profiles for the polymer  
26 repeat units and the benzene and n-heptane molecules have been calculated in the  
27 following manner: A thin slice of a few Å thickness cut perpendicular to the z-axis of  
28 the model is moved through the model along the z-axis with a small step-width (a few  
29 tenth of an Å). In each slice the centroids of polymer repeat units and the respective  
30 centroids of benzene and n-heptane molecules are counted. The resulting density  
31 distribution functions are averaged over a large number of snapshots taken for the  
32 model geometry during the MD simulations. There, due to statistical problems the  
33 averaging can only be performed until a certain number of feed molecules has been  
34 absorbed in the polymer.  
35  
36  
37  
38  
39  
40  
41  
42  
43  
44  
45  
46

47  
48 [Insert Figure 4 about here]  
49

50 Figure 4 contains the respective density profiles for the PDMS-1 and PMPHS-1 models.  
51 It can clearly be recognised that in the case of PDMS the simulated initial adsorptive  
52  
53  
54  
55

1  
2  
3  
4 behaviour does not indicate any significant preferential permeation of either one feed  
5  
6 component through this polymer. This is the same result as it was found experimentally  
7  
8 [276].

9  
10 Now the principle of similarity would suggest that the situation towards a more  
11  
12 preferred benzene separation would improve if one of the methyl groups in each PDMS  
13  
14 repeat unit would be replaced by a benzene group. That is exactly what is indicated in  
15  
16 the upper part of Figure 4 by the density profile for PMPHS, showing a significantly  
17  
18 preferred benzene adsorption at the polymer surface.

19  
20  
21 Examples for the benzene and n-heptane adsorption on PMMA and some of its  
22  
23 derivatives, however are shown in Figure 5.

24  
25 [Insert Figure 5 about here]

26  
27  
28 It can be seen that from this point of view and in the series shown, the best separation  
29  
30 effect would be expected for the basic glassy material PMMA. As mentioned before the  
31  
32 reason for this behaviour is most likely an attractive interaction between the carbonyl  
33  
34 groups of this polymer and the  $\pi$ -electrons of the benzene. There are also strong  
35  
36 experimental indications of a preferred adsorption of benzene on PMMA that were for  
37  
38 example observed in adsorption isotherm measurements [287]. PMMA is, however a  
39  
40 very brittle polymer which is not suited for the formation of thin membrane films  
41  
42 needed to measure permeation effects. Therefore several modifications (cf. Figure 1)  
43  
44 were attempted not only to improve the mechanical properties, but also to further  
45  
46 increase the attractive interaction with benzene. But in fact those modifications  
47  
48 obviously lead to a reduction of the carbonyl-benzene interaction, resulting in a  
49  
50 decrease of benzene affinity. Most-likely large ester groups, such as benzyl (PBMA)  
51  
52  
53  
54  
55

and naphthyl (PNMA), "mask" the carbonyl groups of the respective polymers making them inaccessible for local interactions with the benzene molecules of the feed. Consequently, none of these modifications ~~did, lead~~led to a more pronounced initial benzene adsorption in the interface simulations.

#### 4.2 Initial Absorption:

Only in three cases, PMPHS, PMPHSMA and PtBMA the available simulation time of up to 8 ns was sufficient to allow a representative number of feed molecules to become completely absorbed in the polymer part of the respective model (cf. [for the example of PMPHS](#) Figure 6).

[Insert Figure 6 about here]

In these cases it was possible to obtain an estimate for the solubility-related part of the separation factor of the respective polymer for benzene by averaging over a large number of available snapshots of the system taken during the MD simulation:

$\alpha_{\text{benzene/heptane}}$  (cf. Equation 1). There the averaging was performed from the simulation time step at which acceptable convergence of  $\alpha_{\text{benzene/heptane}}$  could be found. For both polymers values of about 2 were obtained after sufficient simulation time. Thus, not even the investigated polymer (PMPHS) with the most preferred initial adsorption of Benzene or the polymer (PtBMA) which showed the fastest initial diffusion (cf. below) did come close to the intended target for an industrial application, which ~~was~~is at about

$\alpha_{\text{benzene/heptane}} = 10$ .

1  
2  
3  
4 Finally some results concerning the model polymer PtBMA, which was expected to  
5 contain an increased amount of free volume (because of the bulky C(CH<sub>3</sub>)<sub>3</sub> substituents)  
6 shall be discussed. As can be seen in Figure 7 already after a relatively short simulation  
7 time penetrant molecules coming in from the left and right hand surface of the polymer  
8 phase almost meet each other in the middle of the polymer layer.  
9

10  
11  
12  
13 [Insert Figure 7 about here]

14  
15  
16 This is the fastest diffusion observed amongst the materials studied (The second fastest  
17 diffusion occurred in PMPHS-1, cf. Figure 6). In addition an effect related ~~with~~to -the  
18 phenomenon, that in pervaporation membranes normally strong differences between  
19 pure and mixed feed transport behaviours (coupling of fluxes) exist, shall be mentioned.  
20 As confirmed by the following PtBMA model simulation results coupling of fluxes can  
21 strongly influence the separation behaviour. Due to the depletion of the feed from n-  
22 heptane and strong polymer swelling (pre-conditioning) the remaining excess  
23 component may be then absorbed preferentially. In about the first ns of MD simulation  
24 time the investigated PtBMA models are n-heptane selective (cf. Figure 7 (top) a and  
25 Table 5), i.e. in this time mostly n-heptane molecules are entering the polymer and  
26 cause local swelling effects. This swelling leads to laterally increased hole sizes which  
27 then permit also a larger number of benzene molecules to enter the model membrane.  
28  
29 As result already after 2 ns the PtBMA is benzene selective (cf. Figure 7 (bottom) b).  
30 Similar effects of one feed component helping the passage of another component are  
31 often found also in gas separation membranes particularly if one of the feed constituents  
32 is CO<sub>2</sub> [298]. In order to compensate such effects in the simulations the depleted feed  
33 has to be “refilled” by substitution of the excess component with the missing  
34 component.  
35  
36  
37  
38  
39  
40  
41  
42  
43  
44  
45  
46  
47  
48  
49  
50  
51  
52  
53  
54  
55

### 4.3 Diffusion mechanism:

In several examples differences in the diffusion behaviour between the conformationally stiff benzene and the conformationally flexible n-heptane could be observed. These effects could be best seen for the two polymer models with the fastest diffusion of penetrants (PMPHS-2 and PtBMA-2). Here, the conformationally flexible n-heptane molecules follow preferentially the course of diffusion channels with a basically continuous diffusion along the voids, while the rigid benzene molecules rather remain in suited voids for up to several hundred ~~nanoseconds~~ picoseconds. Whenever then channels between two adjacent voids are opening jump events become possible, resulting in a "jump-like" diffusion mechanism of benzene similar to the case of small molecules (e.g. H<sub>2</sub>, N<sub>2</sub>, O<sub>2</sub>) in gas separation membranes [2]. This behaviour can be well recognised from graphic displays of a travelled distance  $R(t)$  of a molecule as function of simulation time  $t$ . Figure 8 shows the typical movements of each a representative benzene and n-heptane molecule in glassy PtBMA.

[Insert Figure 8 about here]

Using the simulation data it is also possible to visualise the reptation-like mechanism of individual n-heptane molecules. Figure 9 shows an example where an n-heptane molecule (white colour) is progressing by a transformation from a relatively extended state at a simulation time of 1.725 ns via a highly coiled state in the area of 1.800 ns to again an energetically favourable, extended configuration at 1.900 ns.

[Insert Figure 9 about here]

### 5. Summary:



1  
2  
3  
4  
5  
6 The theoretical approach towards the separation problem of an organic/organic feed  
7  
8 mixture of 20 wt% benzene and 80 wt% n-heptane with dense amorphous polymer  
9  
10 membranes was investigated utilising molecular modelling techniques. It could be  
11  
12 demonstrated that MD simulations of polymer-feed interface models can reproduce at  
13  
14 least qualitatively important experimental results from related membrane pervaporation  
15  
16 processes. For this purpose mainly the initial adsorption of feed molecules at the  
17  
18 polymer surface and the subsequent initial stages of absorption were considered. These  
19  
20 models are therefore suited to obtain a better insight in the mechanisms of pervaporation  
21  
22 on atomistic length scale. For example it was found that both size and electrostatic  
23  
24 properties of ester groups as well as void size and distribution in the polymer strongly  
25  
26 influence the benzene affinity of PMMA derivatives ~~and can even reverse the observed~~  
27  
28 ~~separation tendencies.~~  
29

30  
31 However, all model polymers which were studied as membranes materials for the above  
32  
33 mentioned separation problem did not show a trend to a sufficient selectivity for  
34  
35 industrial applications in the MD simulations. Thus, afterwards laboratory efforts for  
36  
37 chemical synthesis, membrane formation and characterisation of a number of these  
38  
39 materials could be avoided.  
40

41  
42 In addition, the knowledge about the underlying diffusion mechanism ~~could behas been~~  
43  
44 improved. It could be for instance shown that the rigid benzene penetrants diffuse in a  
45  
46 jump-like manner between adjacent holes of the respective polymer matrix while the  
47  
48 flexible n-heptane molecules ~~perform follow~~ a more continuous diffusion style.  
49  
50

## Acknowledgements

We thank Dr. Schwarz (GKSS) and Regine Apostel (GKSS) for the pervaporation measurements on PDMS films and Christine Dannenberg (Technical University of Berlin) for the measured density values. We would like to acknowledge that parts of the work were supported by the European Commission "Growth" Program, "PERMOD – Molecular modelling for the competitive molecular design of polymer materials with controlled permeability properties.", Contract #G5RD-CT-2000-200.

## References

- [1] F. Müller-Plathe. Permeation of polymers - A computational approach. *Acta Polymerica*, **45**, 259 (1994).
- [2] D. Hofmann, L. Fritz, J. Ulbrich , C. Schepers , M. Böhning. Detailed-atomistic molecular modelling of small molecule diffusion and solution processes in polymeric membrane materials. *Macromol. Theory Simul.*, **9**, 293 (2000).
- [3] Y. Tamai , H. Tanaka, K. Nakanishi. Molecular Simulation of Permeation of Small Penetrants through Membranes. 1. Diffusion Coefficients. *Macromolecules*, **27**, 4498(1994).
- [4] Y. Tamai , H. Tanaka, K. Nakanishi. Molecular Simulation of Permeation of Small Penetrants through Membranes. 1. Solubilities. *Macromolecules*, **28**, 2544 (1995).
- [5] F. Müller-Plathe. Diffusion of water in swollen poly(vinyl alcohol) membranes studied by molecular dynamics simulation. *J. Membrane Sci.*, **141**, 147 (1998).

- 1  
2  
3  
4 [6] M. Wesslein, A. Heintz, R.N. Lichtenthaler. Pervaporation of liquid mixtures  
5 through Poly(Vinyl Alcohol) (PVA)-Membranes. I. Study of water containing  
6 binary systems with complete and partial miscibility. *J. Membrane Sci.*, **51**, 169  
7 (1990).  
8  
9  
10  
11 [7] Huang RYM (Ed.). *Pervaporation membrane separation processes*, Elsevier  
12 Science, Amsterdam (1991).  
13  
14  
15 [8] J.M. Watson, G.S. Zhang, P.A. Payne. The diffusion mechanism in silicon  
16 rubber *J. Membrane Sci.*, **73**, 55 (1992).  
17  
18  
19 [9] T.M. Aminabhavi, R.S. Khinnavar, S.B. Harpogopad, Q.T. Nguyen, K.C.  
20 Hansen. Pervaporation Separation of organic-aqueous and organic-organic  
21 binary mixtures. *J. Membrane Sci.-Rev. Macromol. Chem. Phys.*, **C34(2)**, 139  
22 (1994).  
23  
24  
25 [10] J.M. Watson, P.A. Payne. A study of organic compound pervaporation through  
26 silicone rubber. *J. Membrane Sci.*, **49**, 171 (1990).  
27  
28  
29 [11] M. Mulder. *Basic Principles of Membrane Technology*. Kluwer Academic  
30 Publishers, Dordrecht (1991).  
31  
32  
33 [12] L. Fritz, D. Hofmann. Molecular dynamics simulations of the transport of water-  
34 ethanol mixtures through polydimethylsiloxane membranes. *Polymer*, **38**, 1035  
35 (1997).  
36  
37  
38 [13] L. Fritz , D. Hofmann. Behaviour of water-ethanol mixtures in the interfacial  
39 region of different polysiloxane membranes - a molecular dynamics simulation  
40 study *Polymer*, **39**, 2531 (1998).  
41  
42  
43  
44  
45  
46  
47  
48  
49  
50  
51  
52  
53  
54  
55

- 1  
2  
3  
4 [14] D. Hofmann, L. Fritz, D. Paul. Molecular modeling of pervaporation separation  
5 of binary mixtures with polymeric membranes. *J. Membrane Sci.*, **144**, 145  
6 (1998), 145.  
7  
8  
9  
10 [15] G. Malsch (GKSS Research Center). Personal communication.  
11  
12 [16] K. Inui, H. Okamura, T. Miyata, T. Urugami. Permeation and separation of  
13 benzene/cyclohexane mixtures through cross-linked poly(alkyl methacrylate)  
14 membranes. *J. Membrane Sci.*, **132**, 193 (1997).  
15  
16  
17 [17] K. Inui, T. Noguchi, T. Miyata, T. Urugami. Pervaporation Characteristics of  
18 Methyl Methacrylate–Methacrylic Acid Copolymer Membranes Ionically  
19 Crosslinked with Metal Ions for a Benzene/Cyclohexane Mixture. *J. Appl.*  
20 *Polym. Sci.*, **71**, 233 (1999).  
21  
22  
23  
24  
25  
26 [18] K. Kusakabe, S. Yoneshige, S. Morooka. Separation of benzene/cyclohexane  
27 mixtures using polyurethane–silica hybrid membranes. *J. Membrane Sci.*, **149**,  
28 29 (1998).  
29  
30  
31  
32 [19] Molecular Simulations Inc. 1999, Computational results obtained using software  
33 programs from Molecular Simulations Inc. of San Diego-molecular mechanics  
34 calculations from Discover (Version 4.0.0p+) and graphical display using  
35 InsightII., (1999).  
36  
37  
38  
39  
40  
41 [20] H. Sun, S.J. Mumby, J.R. Maple, A.T. Hagler. An ab Initio CFF93 All-Atom  
42 Force Field for Polycarbonates. *J. Am. Chem. Soc.*, **116**, 2978 (1994).  
43  
44  
45 [21] Polymer User Guide Synthia Section, Version 400p+, San Diego: Molecular  
46 Simulations Inc., (1999).  
47  
48  
49 [22] J. Bicerano. Prediction of polymer properties, Marcel Dekker, New-York  
50 (1993).  
51  
52  
53  
54  
55

- 1  
2  
3  
4 | [232] D.N. Theodorou, U.W. Suter. Detailed Molecular Structure of a Vinyl Polymer  
5 | Glass. *Macromolecules*, **18**, 1467 (1985).  
6  
7  
8 | [243] D.N. Theodorou, U.W. Suter. Atomistic Modeling of Mechanical Properties of  
9 | Polymeric Glass. *Macromolecules*, **19**, 139 (1986).  
10  
11  
12 | [254] ABCR- Catalogue 1994/95, Research Chemicals, ABCR GmbH and Co.,  
13 | Karlsruhe, (1994).  
14  
15  
16 | [265] C. Dannenberg (Technical University of Berlin). Personal communication.  
17  
18 | [276] H.H. Schwarz (GKSS Research Center). Personal communication.  
19  
20 | [287] A. Wenzel, H. Yanagishita, D. Kitamoto, A. Endo, K. Haraya, T. Nakane, N.  
21 | Hanai, H. Matsuda, N. Koura, H. Kamusewitz, D. Paul. Effects of preparation  
22 | condition of photoinduced graft filling-polymerized membranes on  
23 | pervaporation performance. *J. Membrane Sci.*, **179**, 69 (2000).  
24  
25  
26  
27  
28 | [298] C. Staudt-Bickl, W.J. Koros. Improvement of CO<sub>2</sub>/CH<sub>4</sub> separation  
29 | characteristics of polyimides by chemical crosslinking . *J. Membrane Sci.*, **155**,  
30 | 145 (1999).  
31  
32  
33  
34  
35  
36  
37  
38  
39  
40  
41  
42  
43  
44  
45  
46  
47  
48  
49  
50  
51  
52  
53  
54  
55

System	Simulation temperature T in K	Polymer density in $\text{g cm}^{-3}$		$T_{g, \text{Synthia}}$ in K
		$\rho_{\text{exp.}}$ at 298K	$\rho_{\text{Synthia}}(T)$	
PDMS	303	0,95 <sup>1</sup>	0,952	154
PMPPhS	303	1,102 <sup>2</sup>	1,108	213
PMMA	303		1,157	355
PBMA	303	1,188 <sup>2</sup>	1,177	385
PNMA	303	-	1,186	406
PAMA	303	-	1,220	419
PtBMA	303	-	0,967	365
PMPPhSMA	303	-	1,040	375
PMPPhSMA	353	-	1,028	375

<sup>1</sup> literature data taken from ref. [254]

<sup>2</sup> measured with the gradient tube method [265]

Table 1: Estimates of densities  $\rho_{\text{Synthia}}$  (plus where available measured values  $\rho_{\text{exp.}}$ ) and glass transition temperatures  $T_{g, \text{Synthia}}$

stage of equilibration	status of p and T	scaling factor for conformation energy terms in the forcefield	type of nonbonded interaction energy terms in the forcefield	scaling factor for atomic radii in nonbonded interaction energy terms	Integration time step in fs
1	NVT 303K	0.001	repulsive 4th order	0.5	0.05
2	NVT 303K	0.1	repulsive 4th order	0.5	0.05
3	NVT 303K	0.1	repulsive 4th order	2/3	0.05
4	NVT 303K	1	repulsive 4th order	1	0.05
5	NVT 303 K	1	6-9 potential + Coulomb	1	0.2
6	NVT 600K	1	6-9 potential + Coulomb	1	0.5
7	NVT 303K	1	6-9 potential + Coulomb	1	1

Table 2: Typical basic equilibration procedures. The individual stages lasted between 1 ps and 5 ps.

Model System	Remarks	Number of Atoms N	Length of z axis for polymer model in Å (x,y = 24,5Å)	Length of z axis for complete polymer-feed model in Å (x,y = 24,5Å)	Simulation temperature in K	Simulation time in ns
Feed-1	benzene / n-heptane (20:80) <sup>1</sup>	1448	26,3	n.a.	303	n.a.
Feed-2	benzene / n-heptane (20:80) <sup>1</sup>	1448	28,5	n.a.	353	n.a.
PDMS	+ Feed-1	2202	47,4	73,7	303	5,0
PMPHS-1	+ Feed-1	2261	45,2	71,5	303	3,5
PMPHS-2	Continuation of PMPHS-1	2261	45,2	71,5	303	5,5
PMMA	+ Feed-1	3000	46,7	73,0	303	3,0
PBMA	+ Feed-1	2592	43,1	69,4	303	5,8
PNMA	+ Feed-1	3100	52,7	79,0	303	4,0
PAMA	+ Feed-1	3700	62,6	88,9	303	3,0
PtBMA-1	+ Feed-1	3052	49,2	75,5	303	1,0
PtBMA-2	+ Feed-1	3052	49,2	75,5	303	3,0
PMPHSMA-1	+ Feed-1	3400	62,3	88,6	303	2,0
PMPHSMA-2	+ Feed-2	3400	63,0	91,5	353	8,0

<sup>1</sup> Feed composition in wt.-%

<sup>2</sup> -all other models were simulated with the peff forcefield

Table 3: Basic data for the utilised polymer and feed models. The simulation time in the last column always is meant for the respective interface model (polymer-feed).



Stage of equilibration	Scaling factor for conformation terms	Scaling factor for nonbond terms
1	0.001	0.001
2	0.1	0.001
3	1	0.001
4	1	0.1
5	1	1

Table 4: Forcefield scaling factors for the feed equilibration procedure. The integration time step was always 1 fs. The 6-9 nonbond pair interaction and the Coulomb potential of the pcff forcefield were applied.

## Figure Captions

Figure 1: Selection scheme for the simulated polymers.

Figure 2: Construction of a 3-dimensional periodic (3D-PBC) interface model from a 2-dimensional periodic (2-D PBC) polymer packing model and a 2-D PBC solvent packing model (Example PDMS and benzene/n-heptane).

Figure 3: Representative view of the PMPHS-1 interface model after 0.1 ns MD simulation. Light grey = Polymer, dark grey = n-heptane, black = benzene. The long axis of the model is directed along the z-axis.

Figure 4: Normalised density profiles for polymer repeat units (thin grey line), benzene molecules (black line) and n-heptane molecules (thick grey line) as functions of the z-coordinate (in Å) of the PDMS and PMPHS-1 interface models (cf. Figure 3). PDMS was averaged over 5 ns while PMPHS-1 was averaged over 0.3 ns

Figure 5: Normalised density profiles for polymer repeat units (thin grey line), benzene molecules (black line) and n-heptane molecules (thick grey line) as functions of the z-coordinate of the respective interface model (cf. Figure 3). PMMA averaged over 1 ns, PBMA and PBNA averaged over 2 ns

Figure 6: Representative view of the PMPHS-1 interface model after 5.5 ns MD simulation. Light grey = Polymer, dark grey = n-heptane, black = benzene. The long axis of the model is directed along the z-axis.

Figure 7: Representative view of the PtBMA-2 interface model after 1 ns (top) and after 2 ns (bottom) MD simulation. Light grey = Polymer, dark grey = n-

1  
2  
3 heptane, black = benzene. The long axis of the model is directed along the z-  
4 axis.  
5  
6

7  
8 Figure 8: Displacement  $\mathbf{R}(\mathbf{t})$  vs. simulation time  $\mathbf{t}$  for a typical benzene and a typical n-  
9 heptane molecule in PtBMA.  
10

11  
12 Figure 9: Slithering move of a n-heptane molecule in PtBMA shown in a 5 Å thick slice  
13 cut out of the PtBMA-2 model perpendicular to the x-axis direction. Black =  
14 Polymer, light grey = n-heptane molecule of interest, grey = other n-heptane  
15 and benzene molecules.  
16  
17  
18  
19  
20  
21  
22  
23  
24  
25  
26  
27  
28  
29  
30  
31  
32  
33  
34  
35  
36  
37  
38  
39  
40  
41  
42  
43  
44  
45  
46  
47  
48  
49  
50  
51  
52  
53  
54  
55  
56  
57  
58  
59  
60